ANALYTICAL MODELING OF WOOD FRAME SHEAR WALLS SUBJECTED TO VERTICAL LOAD

A Thesis

by

HAI NGUYENDINH

Submitted to the Office of Graduate Studies of
Texas A&M University
in partial fulfillment of the requirements for the degree of

MASTER OF SCIENCE

May 2011

Major Subject: Civil Engineering

Analytical Modeling of Wood Frame Shear Walls Subjected to Vertical Load

ANALYTICAL MODELING OF WOOD FRAME SHEAR WALLS

SUBJECTED TO VERTICAL LOAD

A Thesis

by

HAI NGUYENDINH

Submitted to the Office of Graduate Studies of
Texas A&M University
in partial fulfillment of the requirements for the degree of

MASTER OF SCIENCE

Approved by:

Chair of Committee,	Monique Hite Head
Committee Members,	Luciana R. Barroso
	Junathala Reddy
Head of Department,	John Niedzwecki

May 2011

Major Subject: Civil Engineering

ABSTRACT

Analytical Modeling of Wood Frame Shear Walls

Subjected to Vertical Load. (May 2011)

Hai Nguyendinh, B.S., Hanoi University of Transport and Communication

Chair of Advisory Committee: Dr. Monique Hite Head

A nonlinear automated parameter fitted analytical model that numerically predicts the load-displacement response of wood frame shear walls subjected to static monotonic loading with and without vertical load is presented. This analytical model referred to as Analytical Model of wood frame SHEar walls subjected to Vertical load (AMSHEV) is based on the kinematic behavior of wood frame shear walls and captures significant characteristics observed from experimental testing through appropriate modeling of three failure mechanisms that can occur within a shear wall under static monotonic load: 1) failure of sheathing-to-framing connectors, 2) failure of vertical studs, and 3) uplift of end studs from bottom sill. Previous models have not accounted for these failure mechanisms as well as the inclusion of vertical load, which has shown to reveal beneficial effects such as increasing the ultimate load capacity and limiting uplift of the wall as noted in experimental tests. Results from the proposed numerical model capture these effects within 7% error of experimental test data even when different magnitudes of vertical load are applied to predict the ultimate load capacity of wood frame shear walls.

ACKNOWLEDGEMENTS

I would like to express my deepest gratitude to my advisor, Dr. Head, for her guidance and support during my time at Texas A&M University. Thank you, Dr. Head, for your patience guiding me throughout this research. It’s you who has helped me understand the essential work of a researcher, which will help me through the path of my scientific career.

I would also like to thank my committee members, Dr. Barroso and Dr. Reddy, for their guidance and support. I also want to extend my gratitude to Dr. Henrry W. Shenton and Peter Dean, whom I have never met, for making a great experimental report that helped me so much in this research. I thank my friends and colleagues and the department faculty and staff for making my time at Texas A&M University a great experience.

I would also like to thank my professors and colleagues at Hanoi University of Transportation and Communication for the very first lessons I have learned as a student and scholar. Thanks to the Vietnamese International Education Department for their financial support in this program.

Finally, thanks to my mom, dad and the whole family for their love, patience and warm encouragement. Thank God for helping my whole family stay healthy and strong.

TABLE OF CONTENTS

CHAPTER Page

LIST OF FIGURES

LIST OF FIGURES

LIST OF TABLES

CHAPTER I

INTRODUCTION

1.1 Motivation

Wood frame structures are widely used for low-rise residential construction in the United States. Shear walls are considered as the primary means of lateral load resisting systems. Understanding the behavior of shear walls is critical to achieve proper design and meet construction standards to help prevent failure of wood structures. Within the last decade, a few finite element models and computer programs have been introduced. However, most of the models and computer programs did not allow vertical load to be applied to the wood frame shear walls to access various loading conditions. In other words, by not accounting for the presence of vertical load, most of the previous models do not represent physical loading conditions where dead and live loads on the roof and floors are present. The study herein addresses this gap of knowledge through the development of a numerical model that accurately predicts the response of wood frame shear walls subjected to both lateral and vertical loads. The benefit of this work has broadened the scope of numerical models that can better characterize structural behavior needed for analysis and design of wood frame shear walls.

1.2 Objectives

In order to develop an enhanced and performance-based finite element model that well predicts the response of wood frame shear walls under various loading

This thesis follows the style of *Journal of Structural Engineering*.

conditions, the following objectives are achieved:

a) To develop a model that accurately characterizes the behavior of wood frame shear walls based on kinematic behavior and experimental test results of full-scaled wood frame shear walls subjected to static monotonic load;
b) To numerically investigate the different responses of wood frame shear walls under different loading and support conditions; and
c) To distinguish the failure mechanisms and determine under which condition(s) each failure mechanism may occur.

1.3 Thesis Outline

The format of this thesis is as follows:

- Chapter II contains an overview of previous research that has been proposed on wood frame shear walls. This chapter includes some theoretical/numerical investigations, nonlinear finite element analyses, and experimental studies that have been conducted on wood frame shear walls.
- Chapter III provides details for modeling the wood frame shear walls. A physical description of a wood frame shear wall is introduced. The development of a finite element (FE) model of wood frame shear walls is presented based on preliminary work by Hite (2002) and Johnston (2005). Finally the newly proposed FE model is presented at the end of this chapter.
- Chapter IV presents the analysis results of the new FE model and comparison to experimental test data to verify the accuracy of the new FE

model. A parametric study on the effect of vertical load and presence of hold-down anchors is also included.

- Chapter V summarizes the work and general trends that were revealed by the results. Suggestions for future work are also presented.

CHAPTER II

LITERATURE REVIEW

2.1 Shear Walls in Building Construction

Wood structures have a long history given the availability of wood prior to the existence of reinforcing steel, concrete and masonry materials. A vast majority of low-rise construction and residential dwelling in the United States still consist of wood-framed structures, where wood frame shear walls are used as a primary means of resisting the lateral loads. Lateral loads applied on a shear wall are resisted primarily by the sheathing and are transferred to framing members via sheathing-to-framing connectors. The wood frame shear wall is often bolted to the sills; thus, all the forces induced into the framing members will be transferred to the foundation. Due to the composite action of the sheathing and framing members, the shear walls utilize the high racking strength (or the lateral load resistance) of the sheathing to provide rigidity and reduce deflection against lateral loads. Thus, shear walls are considered an exceptional mechanism of lateral resistance and in fact widely used.

However, significant damage to wood framed structures caused by earthquakes and hurricanes have been recorded such as in the 1994 Northridge Earthquake. According to the Consortium of Universities for Research in Earthquake Engineering (CUREE), 24 out of 25 casualties caused by building damage from the 1994 Northridge Earthquake occurred in wood framed structures (2002). Many other failures in wood framed structures have also recorded hurricanes such as Andrew (1992) or Katrina

(2005). Given these failures, more research has been conducted in order to investigate the behavior of wood framed structures and propose improvements for current design code. Shear walls, as the primary means of lateral load resistance are at the center of interest. This study is motivated by the need for a numerical model that accurately characterizes the response of wood frame shear walls under various loading and support conditions.

2.2 Current Design Practices for Wood Frame Shear Walls

According to the International Residential Code (IBC 2003), there are minimum requirements for shear wall components, including the framing, sheathing, sheathing-to-framing connectors and bolts connecting the bottom plate to the floor. The frame of the wall consists of double top plates, double end vertical studs, single interior studs, and a single bottom plate. The double top plates and double end studs shall consist of two studs, which are similar to an interior stud of the frame. The studs shall be a minimum No. 3, standard or stud grade lumber, except for bearing studs not supporting floors and nonbearing studs. The stud size, height and spacing shall be in accordance with Table R602.3(5) (IRC-2003). For the stud size of “2 x 4” (grade No. 2, which is higher than minimum requirement of studs and often is used), the lateral unsupported height can be a maximum of 10 ft, and maximum spacing when supporting one floor, roof and ceiling is 16 in. The top plates must be double wood plates, with at least equal width to the studs, and shall have a nominal depth of 2 in. The bottom single plate shall have full bearing on a nominal 2 by (1.5 in.) or larger plate or sill with at least equal width to the studs (The true measurement of a “2 by 4” is actually about 1.5 in. by 3.5 in. When the board is first rough sawn from the log, it is a true “2 by 4”, but the drying process and planning of the board reduce it to the finished 1.5 in. by 3.5 in. size. The lumber is then sold as a "2 by 4" because the cost of the drying and machining are figured in). The number and type and the spacing of the fastener required shall be in accordance with Table R602.3(1) (IRC-2003). The fasteners for the top or bottom plate to stud shall consist of two 16d nails. For double studs, 10d nail spaced at 24 in. shall be specified. Sole plate-to-joist or blocking at braced wall panels shall use three 16d nails spaced at 16 in.

2.3 Experimental Investigation Conducted on Wood Frame Shear Walls

Previous experimental investigations of wood frame shear walls subjected to monotonic lateral loading have been studied for the improvement of the numerical model described herein. In 1983, Atherton (1983) conducted 10 experimental tests on 16 x 48 ft wood frame diaphragms sheathed with particleboard. The research explored the effects of the sheathing thickness, nail size and spacing, blocking and sheathing pattern on the strength of the diaphragms. The author concluded that increasing the nail spacing had the largest effect on the wall strength, and blocking (or using hold-down anchor) had a smaller but also significant effect. Cheung et al. (1988) conducted static and free vibration tests to verify a previous nonlinear finite element model. Three different shear wall layouts were tested, and tests showed that the sheathing-to-framing connectors dominate the shear wall behavior. Dinehart et al. (1998) conducted monotonic and cyclic tests to investigate the stiffness and energy degradation of shear walls with respect to cycle. It was determined that the static tests predicted the maximum load of the dynamic tests fairly well, but they were unable to reasonably predict most of the dynamic properties. They also observed that the failure modes of the walls were quite different from the static to dynamic load cases. Dean and Shenton (2004) conducted 10 static monotonic tests to determine the ultimate capacity of wood frame shear walls under lateral loads. The tests showed that the effect of the vertical loads is significant in increasing the wall capacity, while the hold-down anchor only proved to be a great improvement when vertical load is not present. It was also observed that there were three different failure mechanisms (FM) of the shear walls that occur in different loading and support conditions:

1) FM1: failure of the connections between the sheathing and framing: predominant failure mechanism occurred in all specimens that were subjected to vertical load, with or without the presence of hold-down anchors.
2) FM2: failure of the vertical studs in various forms that would be indicative of cracking, splitting or twisting that occurred in the specimens that used hold-down anchors when there was no vertical load. Failure of the connection between the sheathing and framing also occurred in this case; however, more damage of the vertical studs was observed.
3) FM3: uplift of end studs from bottom sill plate when the specimen did not have any hold-down anchors and no vertical load was applied.

Dinehart et al. (2008) conducted cyclic tests on performance of the viscoelastic (VE) gypsum connections and shear walls. The tests showed that the VE polymer improves structural performance while resisting damage when subjected to shear displacement up to 0.7 in. by providing a constant source of energy dissipation. Seaders et al. (2009)

evaluated the performance of the shear walls under monotonic and cyclic loads. The research also reinforced the conclusions by Dean and Shenton (2004) about the effect of vertical load and hold-down anchors, which indicated that dead load (or vertical load) and the presence of hold-down anchors have beneficial effect on ultimate load capacity, and fully anchored shear walls experienced less damage at the connection between the vertical studs and bottom plate.

2.4 Numerical Modeling of Wood Frame Shear Walls

While shear walls are important structural elements, documented numerical modeling efforts of wood frame shear walls that accurately predict its behavior is limited. One of the reasons for this limitation is because previous models only accounted for FM1. This can be seen easily as the only input data for all previous models besides the elastic modulus and geometric parameters is the load-displacement curve of the sheathing-to-framing connectors (which is also referred to as the connector properties) without regard to FM2 and FM3, which account for the damage of vertical studs and uplift of end studs. For example, Itani and Cheung (1984) created a finite element (FE) model to predict the behavior of wood frame shear wall. The input data for the nonlinear nail element was based on measured load-slip properties. Foschi (1977) analyzed four basic structural components of wood diaphragms: 1) cover; 2) frame; 3) connections between the frame members; and 4) cover-frame connections. An example will be presented in the modeling chapter of this thesis to show that Foschi’s formula does not provide an accurate account of the load-displacement curve of wood frame shear walls up to the ultimate load. In 1991, Dolan and Foschi developed a FE model that included nonlinear connectors, bearing effects between sheathing, and out-of-plane bending of sheathing. The model was compared with the results of static test, and they concluded that the model predicted stiffness well, but the ultimate load was only in fair agreement. In later research, White and Dolan (1995) developed a FE program, WALSEIZ, capable of performing a nonlinear analysis of a wood frame shear wall subjected to monotonic or dynamic loads. The computed results were compared with experimental data to validate the program, which was in favorable agreement. Folz and Filiatrault (2001) also developed a computer program written in ANSI FORTRAN 77 named CASHEW (Cyclic Analysis of SHEar Walls). The shear wall model incorporated in the program can predict the static monotonic and hysteretic load-displacement response and energy dissipation characteristic of wood frame shear walls for the case when there is no vertical load and with the presence of hold-down anchors. However, CASHEW program also only accounted for FM1, as the only input data needed to run CASHEW are the properties of the sheathing-to-framing connecters and the elastic modulus of the sheathing.

Although some experimental research has acknowledged the effect of the vertical loads on the shear wall performance, little has been done to include this effect in a numerical or finite element (FE) model. Hite (2002) developed a FE model to characterize the nonlinear behavior of a wood frame shear wall subjected to combined lateral load and vertical loads. However, the model result was not consistent with the experimental test data reported by Dean and Shenton (2003). Thus, in later research, Johnston (2005) used Hite’s model as the basis, and applied several modifications to try to make better agreement with Dean’s experimental test data. Some of the modifications Johnston made were reasonable, and really were a good effort to account for the real test conditions and phenomena observed. However, the model result still showed a significant difference up to 50% in ultimate load capacity with Dean’s (2003) experimental test data. This suggests that further modifications to Johnston’s model should be made to better predict the behavior of the wood frame shear wall. In order to accurately predict the shear wall behavior in all load cases, Hite’s (2002) model and some of Johnston’s (2005) modifications are used as a basis to develop the FE model described herein that accurately predicts the behavior of wood frame shear walls subjected to various load cases by accounting for all three failure mechanisms. The development of the model and results of analysis are presented in this thesis.

CHAPTER III

ANALYTICAL MODELING OF WOOD FRAME SHEAR WALLS

3.1 Previous Work

This chapter provides background information on the nonlinear finite element (FE) model of the shear wall developed by Hite (2002) and some ideas of modifications to Hite's model discussed by Johnston (2005), which is the foundation of the work herein. Based on the previous work, new modifications are assessed and implemented in order to calibrate the FE model based on the experimental test data conducted by Dean (2003).

3.1.1 Test Specimens and the Schematic of the Finite Element Model of Wood Frame Shear Walls

Hite's model was developed based on the setup of static tests performed in the laboratory by Dinehart (1998). The test specimens had overall dimensions of 8 ft by 8 ft; a sketch of the test specimen is shown in Figure 1. The wall consisted of its framing, sheathing, and nail fasteners. The framing members were No. 2 Spruce-Pine-Fir (SPF) "2 by 4" studs, spaced at 16 in. on center. The framing members comprised of studs also formed a double top plate, single bottom plate, and double-stud end posts of the shear wall. The double-stud end posts were nailed on both sides using 12d nails spaced at 12 in. on center, causing it to behave much like a monolithic member. The vertical studs were end-nailed to the top and bottom plates using two 16d nails. The sheathing consisted of four-ply 15/32 in. BC plywood oriented in the vertical direction, (where B & C correspond to the grade of the veneer on each side of the plywood). The 8d nail fastener spacing was 4 in. along the perimeter and 12 inches in the field.

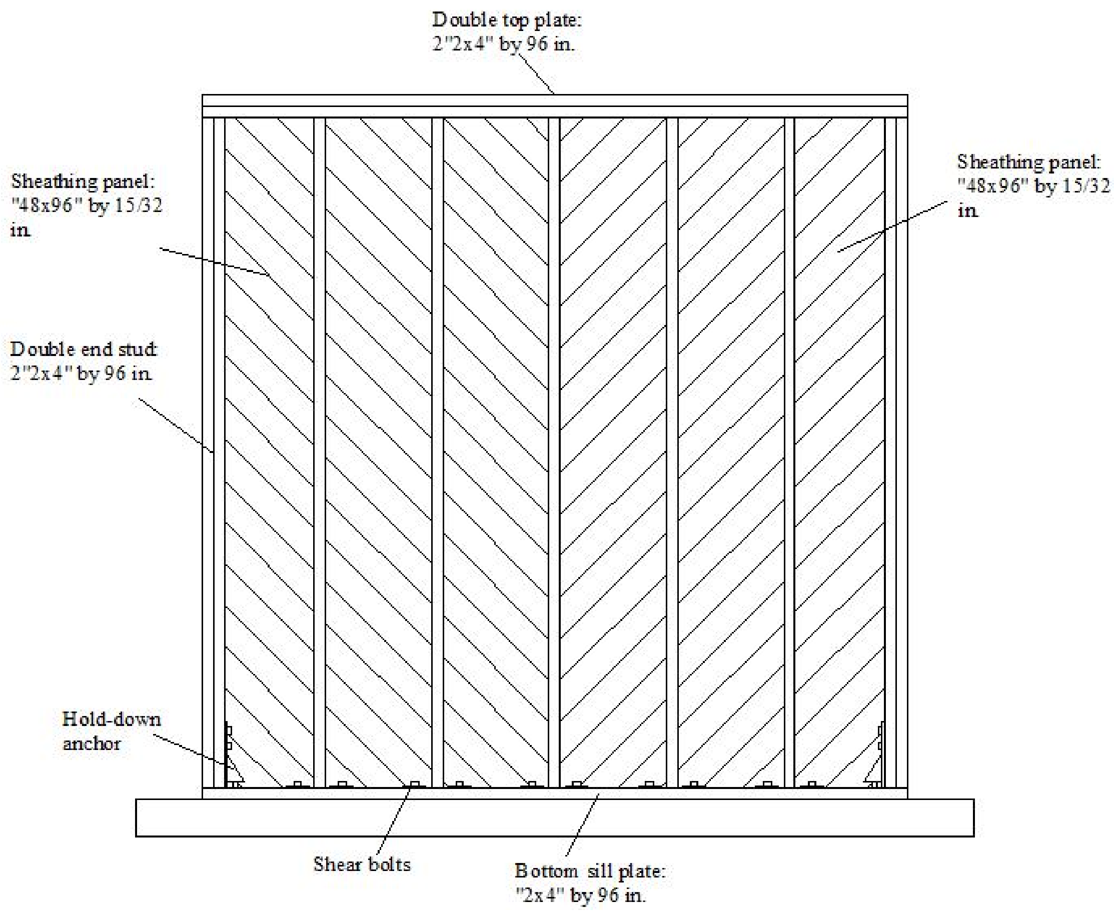

Figure 1: Shear wall construction

The wood frame shear wall was connected to the foundation using 2 hold-down anchors and ten ¾ in. shear bolts along the bottom of the wall. The ten shear bolts exceeded the minimum code requirements for the wall but were used in the test setup to ensure that the wall did not slip on the foundation during testing. Commercially available hold-down anchors were used to resist the uplift forces. The anchors were bolted to the end posts using two ¾ in. through bolts. Another ¾ in. through bolt extended from the foundation where it was bolted through the bottom plate and connected to the hold-down anchor.

Figure 2 shows a schematic of the overall model from Hite's thesis (2002), which Johnston (2005) also used in her thesis. It was created using the commercial finite element program, ANSYS 7.1©. The details of the sheathing, framing, framing-to-sheathing connectors, hold-down anchor and support conditions are as follows.

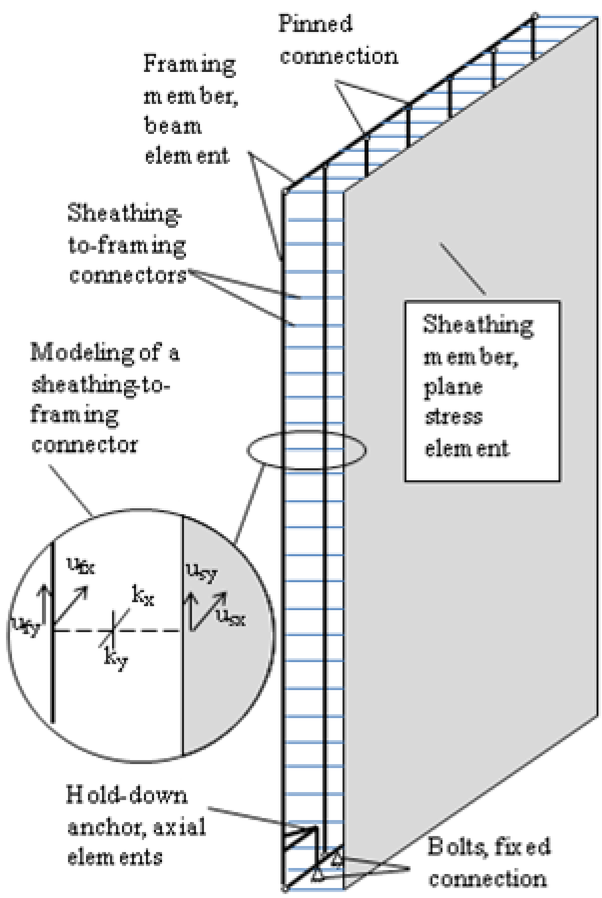

Figure 2: Schematic of the finite element model of shear wall

3.1.2 Modeling of the Sheathing

Johnston (2005) used the same modeling of the sheathing as in Hite's thesis (2002). The PLANE42 elements available in ANSYS© was used by Hite (2002) to model the sheathing member and. It is a 2D plane stress structural solid member as shown in Figure 3. The PLANE42 is used based on the assumption that the sheathing is subjected to mostly in-plane shear force, and little out-of-plane movement occurs. The element has four nodes and two degrees of freedom at each node with translations in the x- and y- directions. It was prescribed with a constant thickness of 15/32 in. and placed in the z = 0.984 in. plane. This distance represents the difference in the locations of the centroids between the framing and sheathing members. The sheathing panels were meshed into approximately 600, 4-in.by 4-in. elements. There is a gap of 0.75 in. between the two panels which accounts for the distance between the centroids of the two nail columns at the edge of the sheathing panels. Poisson's ratio, ν = 0.3, was held constant for the sheathing material during the entire study along with the elastic modulus of E = 234,000 psi.

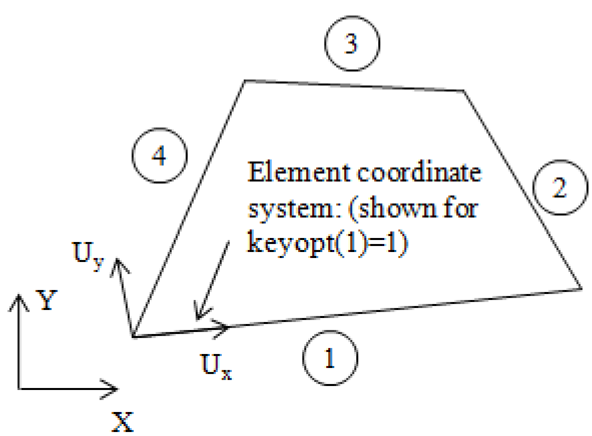

Figure 3: PLANE42 element geometry

3.1.3 Modeling of the Framing

Except for the modification of the geometry of the double top plate, Johnston (2005) used the same model of the framing as in Hite's thesis (2002). The framing was modeled as 2D elastic beam, using the BEAM3 element available in ANSYS©. BEAM3 element has 2 nodes and 3 degrees of freedom at each node with translations in x- and y- directions and rotation about z-axis as shown in Figure 4. The model consists of totally 217 BEAM3 elements. At the intersection of two framing members (i.e. between the stud and top plate and between the stud and bottom plate), there are coincident nodes that provide two nodes at the same location. One node represents the end of a stud and the other one represents the top or bottom plate. The nodes at these joints were coupled in both the x-and y-directions to represent fasteners connecting the two members. In this way, the connections behave like pinned connections as previously shown in Figure 2.

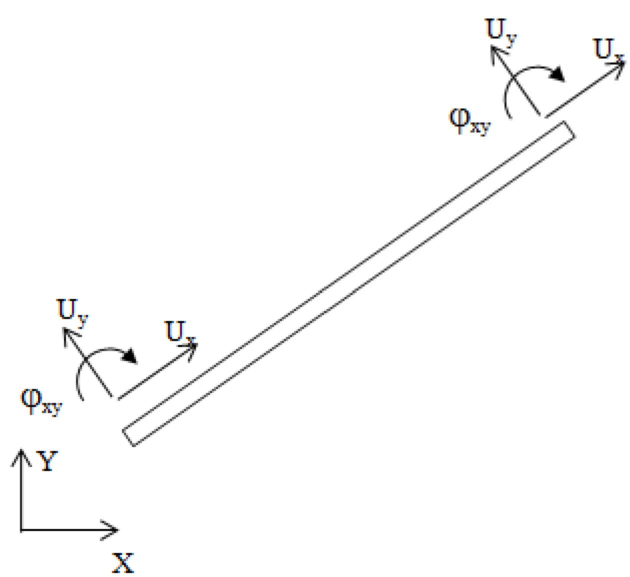

Figure 4: BEAM3 element geometry

The geometric properties were held constant throughout the study. The cross-sectional area of a single “2 by 4” is 5.25 in^2. Depending on the location and number of “2 by 4”s in a member, the cross-sectional area and moment of inertia varies. The interior single studs have a cross-sectional area, A = 5.25 in^2 with a moment of inertia, I = 0.984 in^4 and a height, h = 1.5 in. The double end posts, however, are made up of two “2 by 4” studs with geometric properties as follows: A = 10.5 in^2, I = 7.875 in^4 and h = 3 in. In Hite’s thesis, the double top plate which consisted of two “2 by 4” studs was mistakenly assigned geometric properties A = 10.5 in^2, I = 0.984 in^4, and h = 1.5 in. Johnston (2005) made the correction for the double top plate properties which is used in this thesis. The cross sectional properties of the double top plate were changed to A = 10.5 in^2, I = 7.875 in^4, and h = 3 in. The material properties for the framing members were constant with Poisson’s ratio equal to 0.3 and the elastic modulus equal to E= 1,200,000 psi.

3.1.4 Modeling of the Sheathing-to-framing Connectors

To model the sheathing-to-framing connectors, Johnston (2005) kept the same type of elements as in Hite’s thesis (2002) but modified the element properties. In Hite’s thesis, each nonlinear sheathing-to-framing connector is modeled as two nonlinear springs in the x- and y- directions, denoted in Figure 2 as k_x and k_y for the stiffness of the springs. Translation in x- and y- directions for the sheathing and framing nodes are u_{sx} and u_{sy}, and u_{fx} and u_{fy}, respectively. COMBIN39 element available in ANSYS© is used for both nonlinear springs in x- and y- directions. There are 172 locations for a total of 344 nonlinear spring elements in the corresponding model. Figure 5 shows the sheathing-to-framing connector locations for both models.

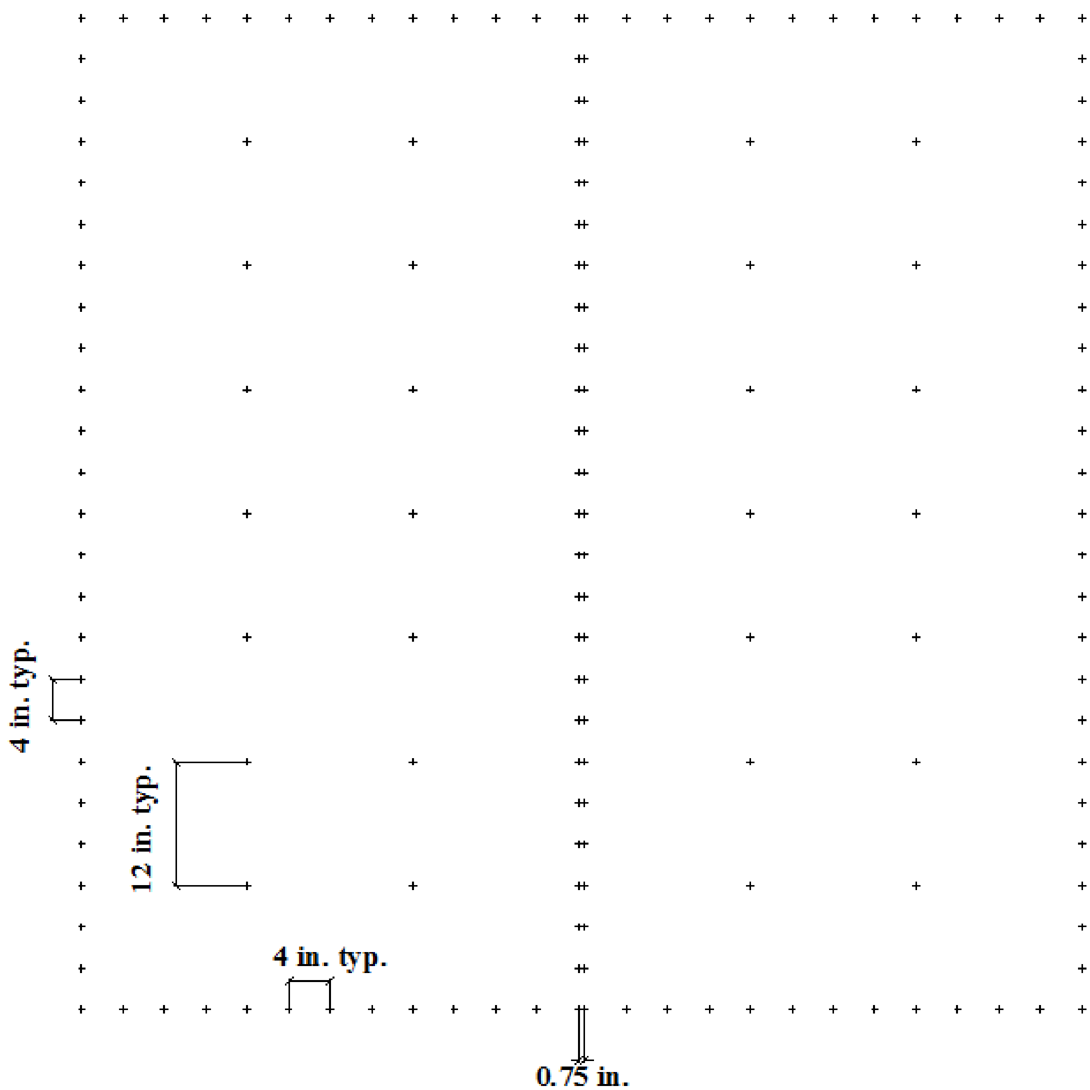

Figure 5: Sheathing-to-framing connector locations

COMBIN39 is a unidirectional element with nonlinear generalized load-displacement capability that can be defined in piecewise segments. In this case, the longitudinal option provides a uniaxial tension-compression element with up to three degrees of freedom at each node: translations in the nodal x-, y-, and z- directions. No bending or torsion is considered. Figure 6 shows the geometry and generalized load-displacement behavior of the COMBIN39 nonlinear spring element.

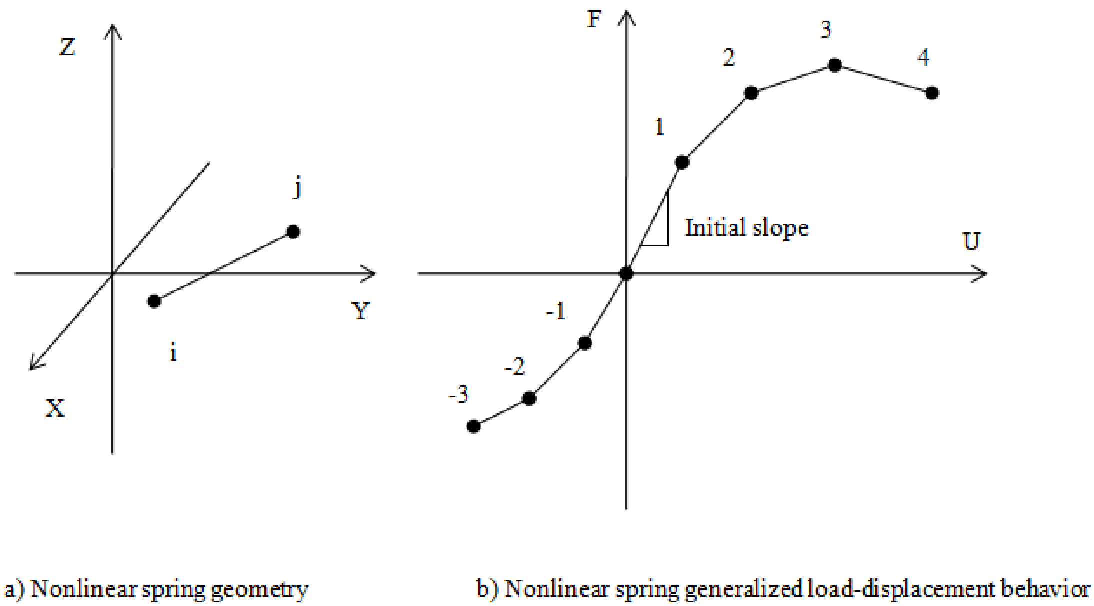

Figure 6: COMBIN39 element geometry

To determine the load-displacement curve of the nonlinear sheathing-to-framing connectors, static tests were conducted on several nailed wood specimens and the defined load-displacement curve is supposed to be the "average curve" of the data zone. Figure 7 shows the tests result and the the load-displacement curves for the sheathing-to-framing connector properties suggested by Hite (2002) and Johnston (2005), which are labeled as "Hite's average curve (2002)" and "Johnston's average curve (2005)." In "Hite's average curve (2002)," the slope of the last segment of the curve was greater than the initial slope. This did not meet ANSYS© requirement for the COMBIN39 element properties. "Johnston's average curve (2005)" met the

ANSYS© requirement for the COMBIN39 element properties, however, was not accurate as it was far from the average zone of the test data. A newly proposed load-displacement curve for the sheathing-to-framing connector properties will be presented in subsection 3.2, new developments of the finite element model. Table 1 and 2 shows the key points for “Hite’s average cuve (2002)” and “Johnston’s average curve (2005).”

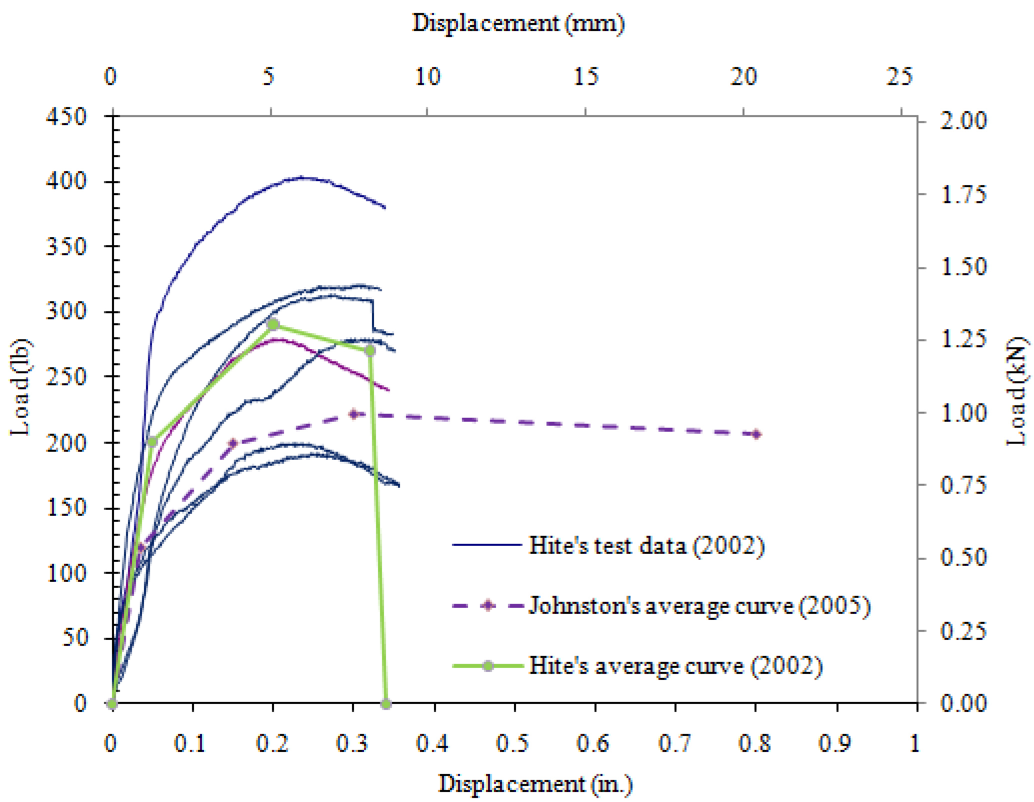

Figure 7: Load-displacement curves by Hite (2002) and Johnston (2005)

Table 1: Sheathing-to-framing connector properties by Hite (2002)

U_x (in)	F (lbs)
0	0
0.05	200
0.2	290
0.32	270
0.34	0
5	10

Table 2: Sheathing-to-framing connector properties by Johnston (2005)

U_x (in)	F (lbs)
0	0
0.035	120
0.15	200
0.35	222.3
0.8	207
2	0
5	10

3.1.5 Support Conditions

When hold-down anchors were applied to the model, Hite used only one, placed at the left end of the structure to prevent uplift on the side where lateral load was applied. Notice that the real specimens had two hold-down anchors on both sides as shown in the Figure 1. Because in reality, the lateral loads caused by winds or earthquakes can come from any of the left or the right side of the shear wall, so the anchors must be installed on both sides. And as the shear wall is symmetric about the vertical central axis, when the lateral load comes from the right, the shear wall behavior will be just the same as when the lateral load comes from the left. Thus, the model only needs one anchor for the case when lateral load comes from the left, as the hold-down on the right side would have no effect on the wall behavior when lateral load comes from the left.

Hite (2002) modeled the hold-down anchor by three axial bars using LINK1 element in ANSYS© as shown in Figure 8a. However, Johnston (2005) noticed that upon analysis of Hite's model of the shear wall under vertical load, the LINK1 element of the hold-down anchor went into compression. This is not true to actual conditions and therefore Johnston modified Hite's model of the hold-down anchor by using LINK10, a "tension only" element available in ANSYS© for the vertical component of the hold-down anchor. The new model of the hold-down suggested by Johnston as shown in Figure 8b is also used in this thesis. Both LINK1 and LINK10 elements have two nodes and two degrees of freedom at each node: translations in the x-and y-directions. The elastic modulus for the two non-vertical members of the hold-down is defined as 1×10^9 psi, in order to form a very stiff truss. The vertical component of the hold down anchor has the elastic modulus of steel, E = 29,000,000 psi and cross-sectional area, A= 0.4418 in^2, corresponding to the 19 mm diameter steel bolt used in the hold-down anchor.

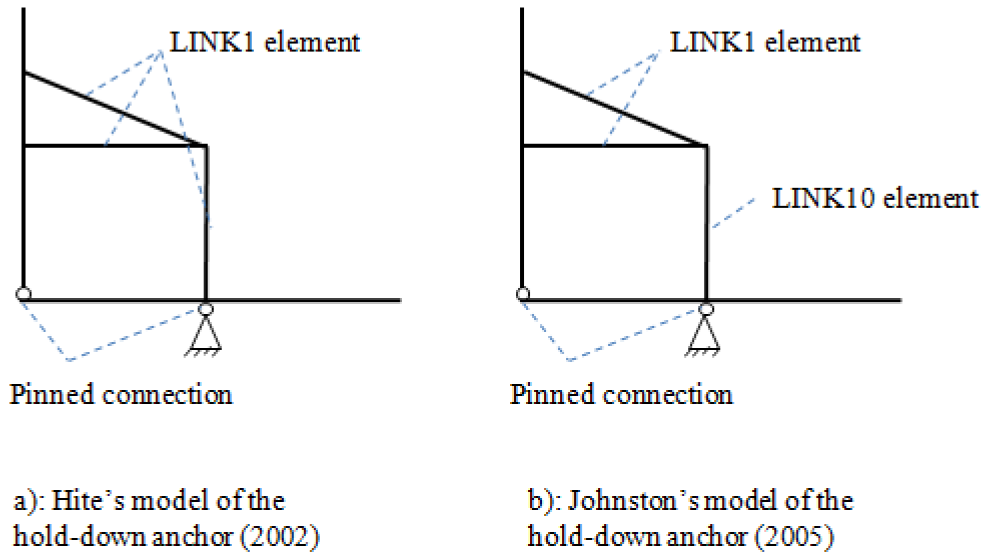

Figure 8: Modeling of the hold down anchor

In Hite's model (2005), at the location of the shear anchor bolts, the framing nodes along the bottom of the wall were restrained in both the x-and y-directions. Where the studs meet the sill plate and in between the shear anchor bolts, additional pinned supports in the y-direction were placed to prevent the sill plate from displacing below the foundation. The support condition is displayed in Figure 9. Note that small circles represent pinned connections and hold-down anchor is not included.

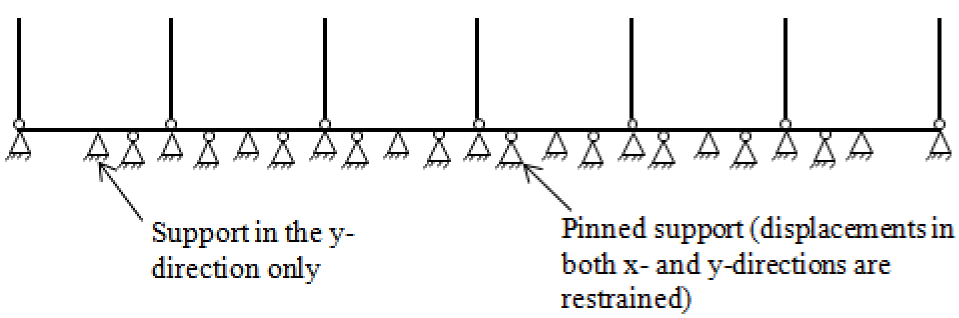

Figure 9: Support condition (Hite 2002)

Johnston (2005) kept the same support condition as in Hite’s model (2005) for the cases when there is vertical load. However, for the cases when there is no vertical load, Johnston removed the y-supports at the bottom of some specific vertical studs which went into tension because that there would not be reaction force from the foundation at the bottom of those vertical studs. However, Both Hite’s model and Johnston’s modification of the support condition did not reflect the physical condition of the real test specimen, which is shown in Figure 1. From Figure 1, it can be seen that the framing member was connected to the foundation through the hold-down anchors and ten shear bolts only. The vertical studs were connected to the bottom sill plate via nailed connections and the bottom sill plate was fixed to the foundations by the shear bolts. At the bottom of the vertical studs and the locations between two shear bolts, there were no connection between the bottom sill plate and the foundation. Thus, the y-supports at the bottom of the vertical studs and between two shear bolts were removed for the newly proposed model addressed in this thesis. The new modeling of the support condition will be presented in subsection 3.2.

3.1.6 Loading

In Hite’s thesis (2002), the vertical load was applied along the top as the surface pressure acting on the upper face of the BEAM3 elements. The 1675 lb/ft vertical load acted in the negative y-direction, yielding a 13,190 lb resultant vertical force. The lateral load, however, was applied in a slightly different manner. To simulate the static loading from the laboratory tests, lateral load was applied by prescribing an incremental displacement at the top left corner of the wall. “The displacement is broken down into several sub-steps, and then ANSYS automatically further divides each sub-step, as it iterates to compute the nonlinear response" (Hite 2002). Johnston (2005) kept the same ways of applying lateral and vertical loads as in Hite's thesis (2002), however, she made a slight modification to the load steps definition in the nonlinear analysis.

In Hite's study (2002), the nonlinear analysis was conducted by breaking one "load step" into two hundred "substeps." This allowed the lateral displacement, at the top left corner of the wall, to be applied in two hundred increments and provided a fairly dense force-displacement response curve for the wall. This is correct for the lateral load. However, Johnston (2005) suggested that in the cases with vertical load, the lateral load was increased after the vertical load had been fully applied. Thus, the lateral and vertical load need to be applied in different load steps in ANSYS©. In load step 1, vertical load as surface pressure was specified as "stepped" and applied to the shear wall model. In load step 2, lateral load was specified as "ramped" with 60 substeps. In this way, lateral load was applied incrementally in 60 substeps after vertical load had been fully applied in only one substep. This modification was correct to describe the real test condition of the shear wall and therefore is also used for the newly proposed model presented in this thesis.

3.2 New Developments

In this thesis, new developments of the finite element (FE) model include the redefinition of the nonlinear sheathing-to-framing connector properties, variations of support conditions, and new model connectivity of the stud-to-bottom plate for the cases without vertical load. The newly proposed model is named as "Analytical Model of wood frame SHEar walls subjected to Vertial load" or AMSHEV. The new developments of the models are as follows.

3.2.1 Redefinition of the Nonlinear Sheathing-to-framing Connector Properties

Figure 10 shows the new definition of the nonlinear sheathing-to-framing connector properties for the FE model presented in this thesis, which is labeled as "Nguyen's average curve (2011)" and plotted in the same graph with "Hite's average curve (2002)," "Johnston's average curve (2005)" and "Foschi curve (1977)."

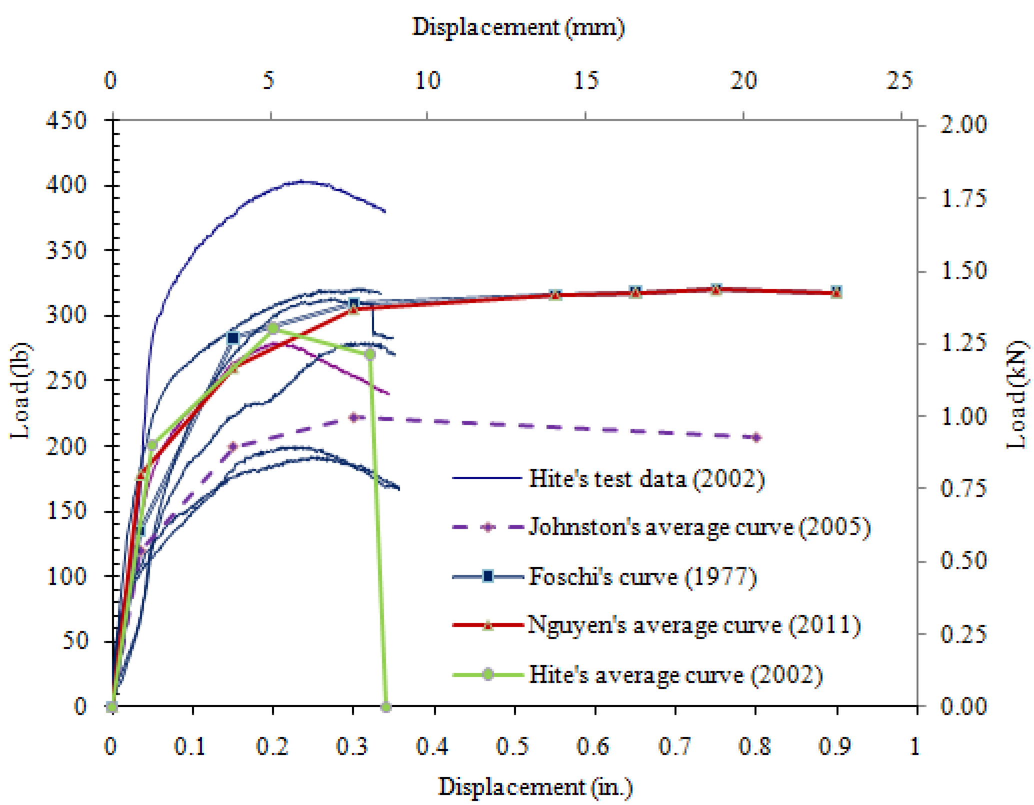

Figure 10: New definition of the sheathing-to-framing connector properties

From Figure 10 it can be seen that there is some variability in the test results. But with many sheathing-to-framing connectors in a shear wall, the total behavior is likely to fall within the average curve of the data zone. “Johnston’s average curve (2005),” however, seems to be much lower than the average zone; thus, further modification of the curve is reasonable and addressed herein. The key points for “Nguyen’s average curve (2011)” are described in Table 3 below.

Table 3: Sheathing-to-framing connector properties by Nguyen (2011)

U_x (in)	F (lbs)
0	0
0.035	178
0.15	260
0.3	305
0.55	316
0.65	318
0.75	320
0.9	318
4	0
10	10

At first, “Foschi’s curve (1977)” was used for the sheathing-to-framing connector properties of the new model, and the predicted ultimate load capacity of the shear wall was shown to be in good agreement with the experimental test data. However, the predicted load-displacement plots of the shear wall showed some discrepancy in the shape of the curve compared to experimental test data (Dean 2003). Thus, some manual adjustment was made from Foschi’s model (1977) to generate the “Nguyen’s average curve (2011).” The points of “Nguyen’s average curve (2011)” were adjusted to better reflect the average zone of the test data from Hite (2002). This enabled the development of the model proposed herein by Nguyen (2011) to predict the behavior of wood frame shear walls in good agreement with experimental test data (Dean 2003).

To see the discrepancy between the shear wall model using “Foschi’s curve (1977)” for the connector properties and experimental test data (Dean 2003) and to show the improvement obtained by using “Nguyen’s average curve (2011),” Figure 11 shows the load-displacement plots for one load case when there is 1700 lb/ft vertical load and with hold-down anchor present. In Figure 11, “Model with Foschi’s curve (1977)” is Nguyen’s model (2011) of the wood frame shear wall using “Foschi’s curve (1977)” for the sheathing-to-framing connector properties. It can be seen from Figure 11 that in the elastic zone, “Model with Foschi’s curve (1977)” was lower than average zone of the test data, while it goes higher than the average zone of the test data in the following part of the curve. “AMSHEV (Nguyen 2011)” using “Nguyen’s average curve (2011)” is shown to give results that are in good agreement when compared to the average experimental test data by Dean (2003).

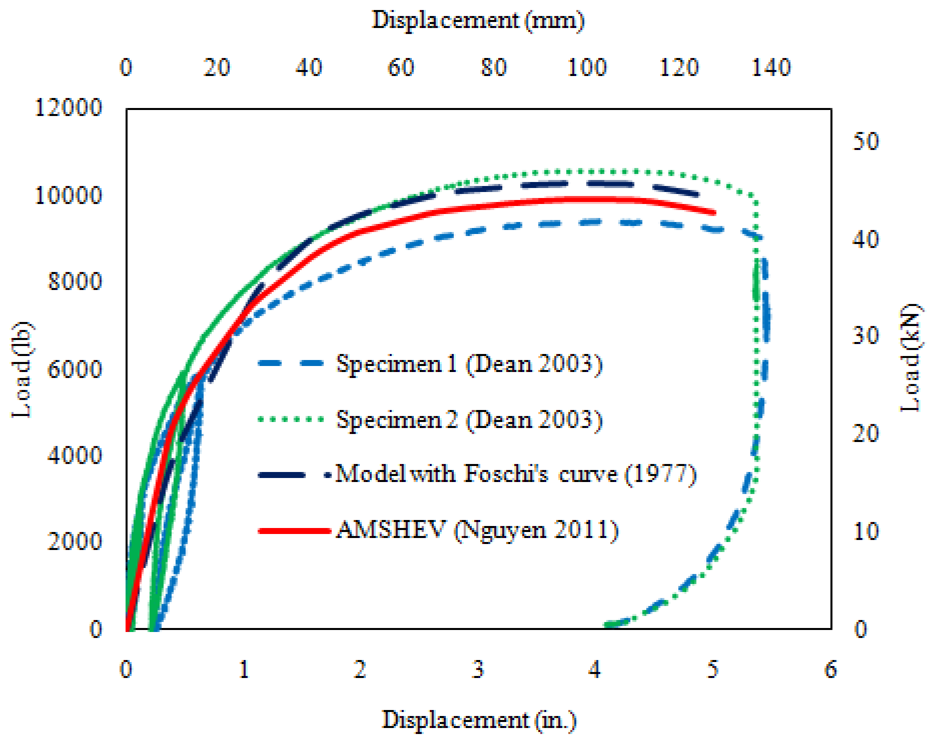

Figure 11: Comparison of predicted load-displacement plots to experimental test data (Dean 2003)

3.2.2 Updated Loading and Support Conditions

The support conditions, or the connections between the vertical studs and the bottom plate, play an important role in predicting the ultimate strength of the shear wall. When there is no vertical load, the tensile stress in the studs caused by the lateral force is larger, thus the studs are more susceptible to failure, where failure is defined as the inability to resist to lateral load. To verify this, three types of analysis were run for all possible load cases with or without vertical load and with or without hold-down anchor: 1) a linear analysis with a lateral load equal to 1417.5 lbs applied to the top, left node of the shear wall; 2) a nonlinear analysis with a lateral load equal to 5200 lbs, which is close to the maximum load capacity for the case when there is no vertical load and no hold-down anchor; and 3) a nonlinear analysis with a lateral load equal to 7400 lbs, which is close to the maximum load capacity for the case when there is no vertical load and with hold-down anchor. The analysis results of the stress in the seven vertical studs, shown in Figure 1 and numbered from left to right on the shear wall, are shown in Tables 4 through 6 as follows.

Table 4: Axial stress in vertical studs due to lateral load equal to 1417.5 lbs

Load Case	Vertical load (lb/ft.)	Hold-down anchor present	Axial stress in vertical studs (psi)						
			σ_1	σ_2	σ_3	σ_4	σ_5	σ_6	σ_7
1	1700	Yes	-22	-369	-385	-335	-347	-364	-260
2	1700	No	-11	-379	-393	-344	-350	-363	-259
3	0	Yes	-12	**63**	-4	16	21	-33	-129
4	0	No	3	**161**	26	47	31	-38	-156

Table 5: Axial stress in vertical studs due to lateral load equal to 5200 lbs

Load Case	Vertical load (lb/ft.)	Hold-down anchor present	Axial stress in vertical studs (psi)						
			σ_1	σ_2	σ_3	σ_4	σ_5	σ_6	σ_7
1	1700	Yes	-20	-96	-440	-346	-260	-497	-583
2	1700	No	5	**161**	-356	-287	-212	-552	-639
3	0	Yes	-17	**267**	-68	25	120	-142	-465
4	0	No	23	**666**	67	121	200	-218	-545

Table 6: Axial stress in vertical studs due to lateral load equal to 7400 lbs

Load Case	Vertical load (lb/ft.)	Hold-down anchor present	Axial stress in vertical studs (psi)						
			σ_1	σ_2	σ_3	σ_4	σ_5	σ_6	σ_7
1	1700	Yes	-24	**8**	-571	-359	-162	-619	-711
2	1700	No	45	**231**	-390	-270	-150	-628	-719
3	0	Yes	-17	**407**	-187	27	236	-259	-596
4	0	No	31	**774**	47	138	254	-267	-608

(*) the minus sign indicates a compression stress

Boldface indicates instances when the second left stud may be subjected to tensile stress

From Tables 4 to 6, it can be seen that tensile stress occurs very early in the linear regime for the cases when there is no vertical load, with or without hold-down anchor. However, the tensile stresses are not large enough to cause damage to the vertical studs at this magnitude of lateral load. When there is a hold-down anchor, the tensile force in the upper part of the end post vertical stud is transferred through the hold-down anchor to the foundation instead of through the bottom of the end post. Thus, the bottom of the end post goes into compression while the second left stud may be subjected to tensile stress (as denoted by the numbers in boldface). When there is no hold-down anchor, tensile stress is largest in the second end stud because of the location of the shear bolt, which is much closer to the second stud than to the end post. For each case when there is no vertical load, once the lateral load reaches the maximum load capacity of that case, tensile stresses are larger and occur more in the studs than in other cases when there is vertical load. It is well known that wood structures have much smaller tensile resistance than compression strength. Thus, for the cases when there is no vertical load large tensile stresses would cause damage in the vertical studs at the connection with the bottom plate as observed by Dean et al. (2003) and Seaders et al. (2009). This phenomenon is defined as the second failure mechanism (FM2) of the shear wall as previously mentioned. In order to represent the failure of the vertical studs when there is no vertical load, pinned connections are replaced by springs in the x- and y- directions as shown in Figure 12. When there is a hold-down anchor, the vertical studs are restrained from lifting up; thus, all the studs have spring connections in the y-direction. But when there is no hold-down anchor, the two left end studs, which are subjected to high tensile stress, must be released the springs in the y-direction such that the end studs are allowed to lift up. Note that in the newly proposed model, there are only ten pinned supports at the bottom sill plate which account for the ten shear bolts as previously explained.

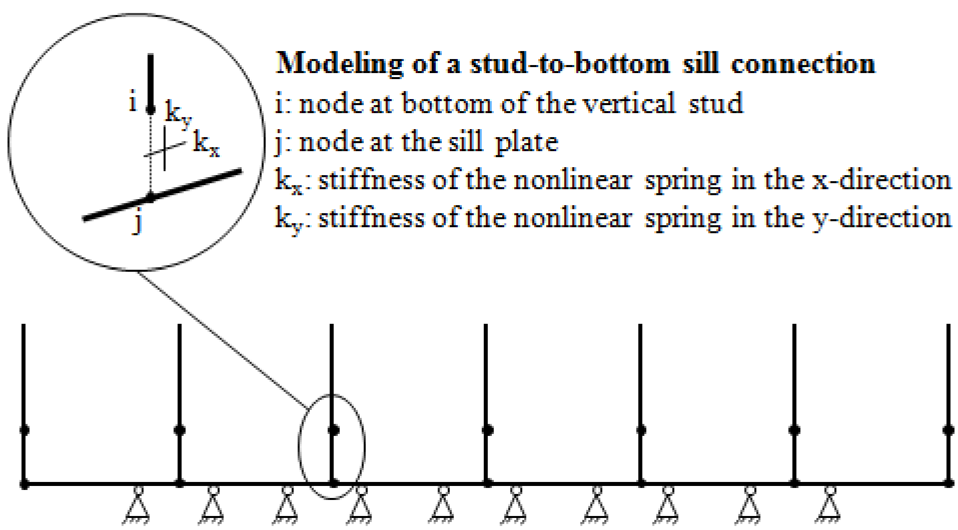

Figure 12: Support condition for the cases without vertical load

The x- and y-direction springs at the stud-to-bottom plate connections are modeled using the same element as the fasteners--the COMBIN39 nonlinear spring. The load-displacement curves for both the springs at the end studs and those of the interior studs were based on the withdrawal strength, thereby mimicking lift-off of the vertical stud and effects on the bottom sill to develop the shape of the curves. As the end studs are different from the interior studs (double to single), the springs have slightly different properties from the exterior compared to interior ones due to the difference in the cross-sectional areas. The properties of the nonlinear springs at the stud-to-bottom plate connections are described in the Tables 7 and 8.

Table 7: End stud spring connector properties

U_x (in)	F (lbs)
0	0
0.035	600
0.2	1800
0.45	2600
0.75	2900
0.9	2850
5	0
12	10

Table 8: Interior stud spring connector properties

U_x (in)	F (lbs)
0	0
0.035	600
0.15	1550
0.35	2250
0.55	2600
0.75	2700
0.9	2650
5	0
12	10

When vertical load is applied, pinned connections are kept for all the stud-to-bottom plate connections, as shown in Figure 13 below.

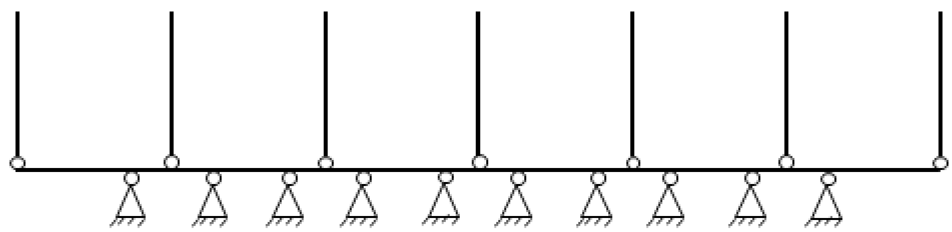

Figure 13: Support condition for the cases with vertical load

Table 9 summarizes the support conditions for all 5 load cases. Notice that in Johnston's thesis (2005), there were only analysis results for 4 loading cases, which are cases 1, 2, 3 and 4 in Table 9. However, in Dean's thesis (2004), there was another experimental result for an additional load case, which is case 5 in Table 9. In this thesis, in order to verify the accuracy of the new FE model (2010), analysis results were compared with experimental test data in all 5 load cases, as shown in Table 9 below. The updated loading and support conditions are the final development of modeling of wood frame shear walls presented in chapter III. In the following, Chapter

IV will present the analysis results and comparison of the new FE model to experimental test data, which verify the accuracy of the FE model.

Table 9: Summary of the updated loading and support conditions

Case	Vertical load (lb/ft.)	Hold-down anchors present	Description of the support conditions	Failure mechanisms (FM)
1	1700	Yes	Pinned connections between the studs and bottom plate	FM1
2	1700	No	Pinned connections between the studs and bottom plate	FM1
3	0	Yes	x- and y- direction springs replace pinned connections at the bottom for all vertical studs	FM1,FM2
4	0	No	x- and y- direction springs replace pinned connections; the two left end studs are released in y- direction	FM3
5	850	Yes	Pinned connections between the studs and bottom plate	FM1

CHAPTER IV

RESULTS OF ANALYSIS

4.1 Load-Displacement Plots

In his MS thesis, Dean (2003) conducted 10 static experimental tests of shear walls with the same dimensions from Dinehart (1998) that were subjected to 5 load cases, as described previously in Table 9. With available data from Dean's experimental tests, the 5 load cases were analyzed with a horizontal displacement applied at the top left corner of the frame. In order to verify the accuracy of the model, the load-displacement curves of the model and the two experimental test specimens are plotted on the same graph. Figures 14, 15, 16, 17 and 18 show the load-displacement plots for all 5 cases. Tables 10, 11, 12, 13 and 14 compare the experimental results to the results obtained from a static nonlinear pushover analysis. In the tables, the three quantities described are the ultimate load, P_{ult}, displacement at ultimate load, $\Delta_{P_{ult}}$, and the effective stiffness, K_E, of the wood frame shear wall.

The effective stiffness of the specimens is calculated by the following formula:

$$K_E = \frac{P_{ult} - P_i}{\Delta_{P_{ult}} - \Delta_i} \tag{4-1}$$

Here P_{ult} is the ultimate load, corresponding to the peak of the load-displacement curve; P_i is the minimum value of the load, which is the initial value, equal to zero; $\Delta_{P_{ult}}$ is the displacement at ultimate load; and Δ_i is the displacement at the initial load, which is equal to zero. The effective stiffness of the model data that is compared to the test data must be calculated at the same location of the end point, which is taken as the average displacement at ultimate load ($\Delta_{P_{ult}-average}$) of the specimens. P_{ult} is replaced by the load of the model data corresponding to ($\Delta_{P_{ult}-average}$) when calculating the effective stiffness of the model.

In the comparison tables, notice that column F denotes the percent difference between the two specimens test results. This column shows that while the ultimate loads of the two specimens are quite close to each other (within 15% difference), the displacement at ultimate load can vary significantly (up to almost 39% difference). Thus, the FE model has been improved with an effort to match the average experimental test results per the ultimate load first. For the displacements at ultimate load, $\Delta_{P_{ult}}$, in some of the cases, the difference between the model and test data is greater than 10%, but notice that the difference between the two specimen results is even higher as reflected in the figures and tables in the following pages.

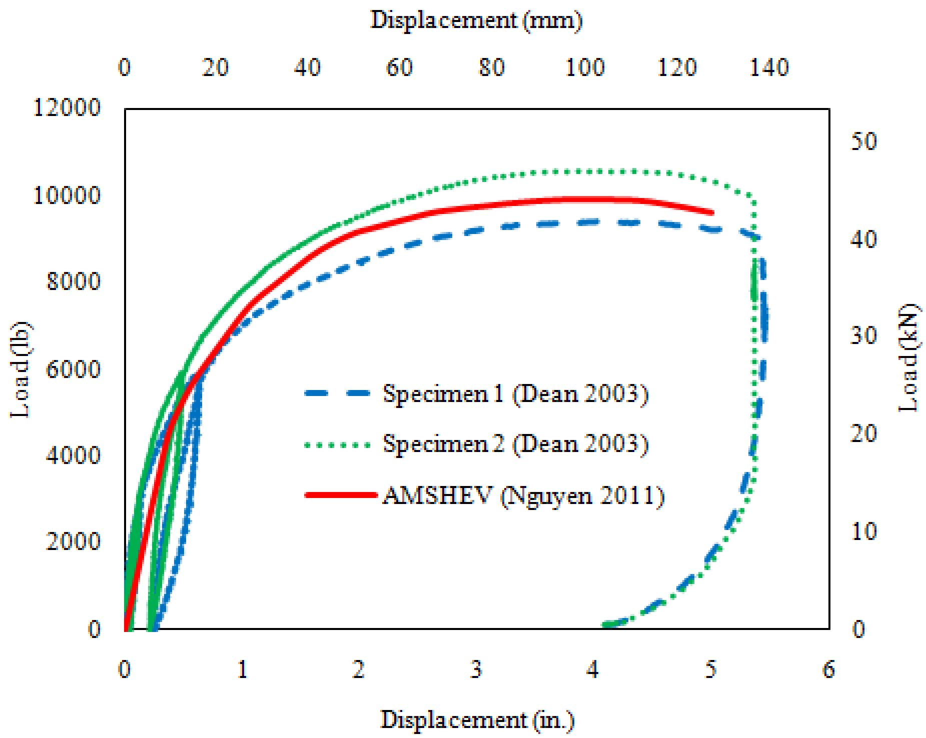

Figure 14: Case 1: With 1700 lb/ft vertical load and hold-down anchor

Table 10: Comparison between AMSHEV and test data for Case 1

	Specimen 1 (A)	Specimen 2 (B)	Difference between A & B (%) (C)	Average test data (D)	AMSHEV (2011) (E)	Difference between D & E (%) (F)
K_E (lb/in)	2656	2339	11.92	2497	2518	0.82
P_{ult}(lbs)	10623	9403	11.48	10013	9918	0.94
$\Delta_{P_{ult}}$ (in)	4.00	4.02	0.50	4.01	3.87	3.49

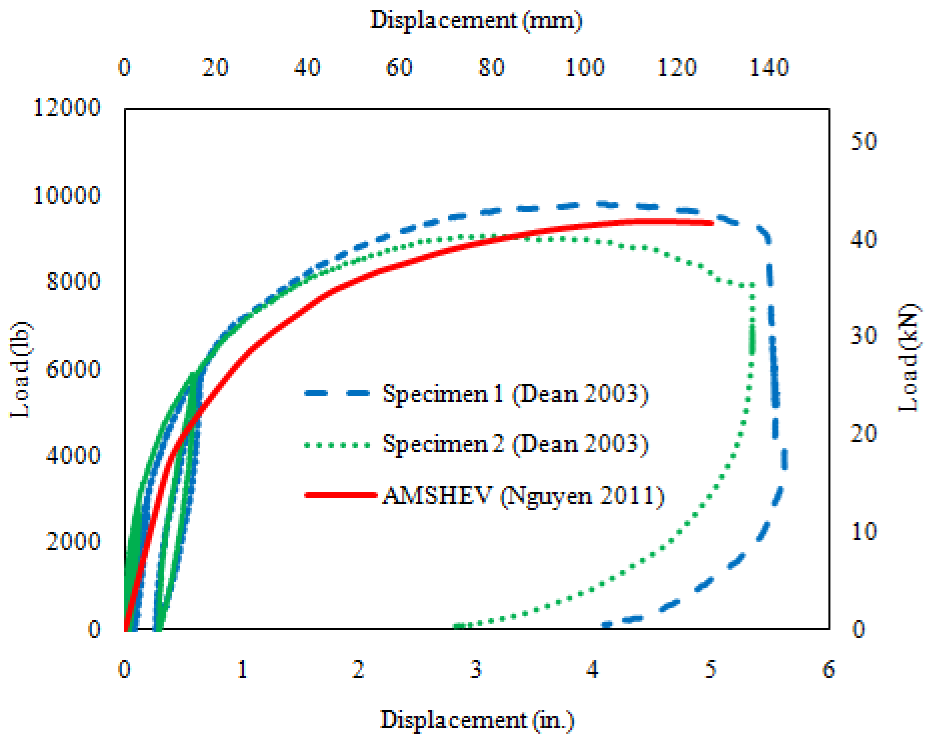

Figure 15: Case 2: With 1700 lb/ft vertical load and no hold-down anchor

Table 11: Comparison between AMSHEV and test data for Case 2

	Specimen 1 (A)	Specimen 2 (B)	Difference between A & B (%) (C)	Average test data (D)	AMSHEV (2011) (E)	Difference between D & E (%) (F)
K_E (lb/in)	2439	3000	23.04	2680	2645	1.29
P_{ult}(lbs)	9803	9061	7.57	9432	9401	0.33
$\Delta_{P_{ult}}$ (in)	4.02	3.02	38.90	3.52	4.46	26.99

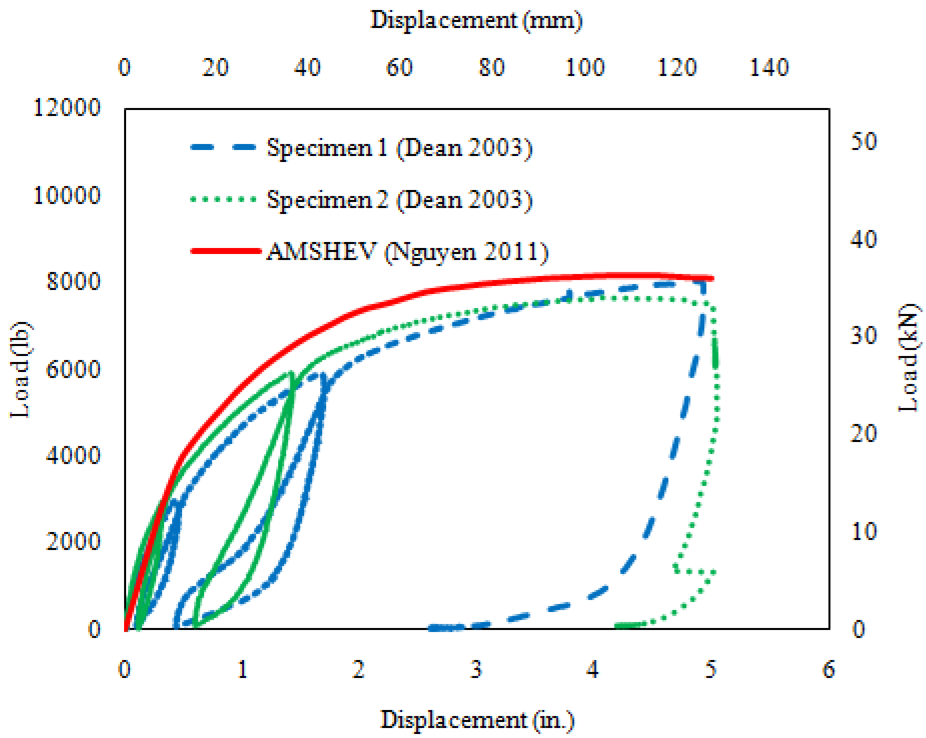

Figure 16: Case 3: No vertical load and with hold-down anchor

Table 12: Comparison between AMSHEV and test data for Case 3

	Specimen 1	Specimen 2	Difference between A & B (%)	Average test data	AMSHEV (2011)	Difference between D & E (%)
	(A)	(B)	(C)	(D)	(E)	(F)
K_E (lb/in)	1646	1890	59.01	1759	1825	3.76
P_{ult}(lbs)	8016	7674	4.27	7845	8147	3.85
$\Delta_{P_{ult}}$ (in)	4.87	4.06	16.63	4.46	4.47	0.15

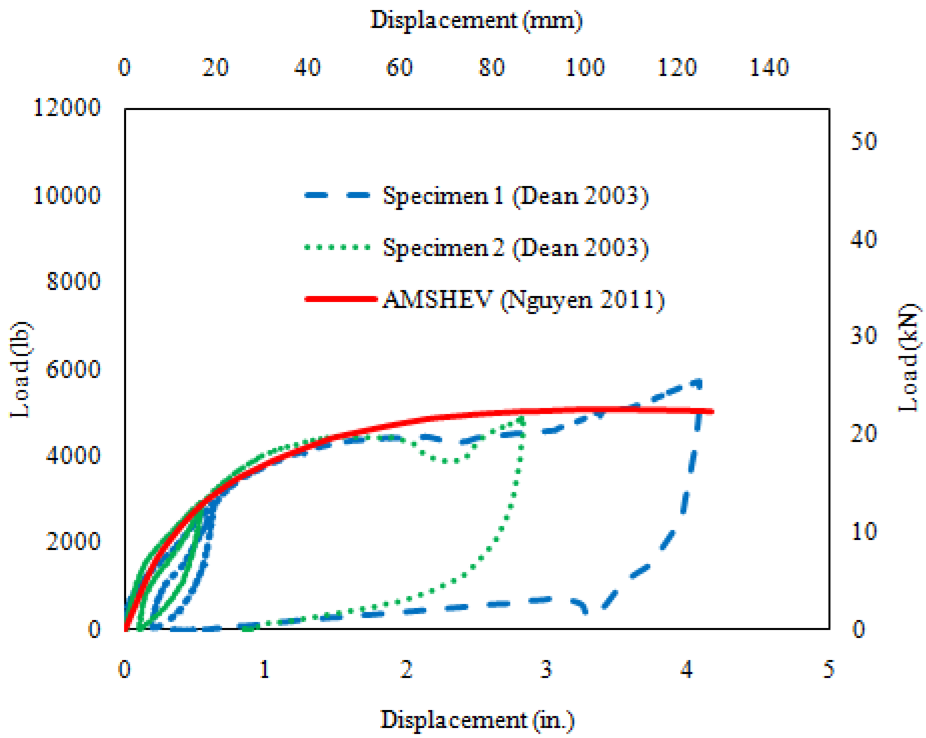

Figure 17: Case 4: No vertical load and no hold-down anchor

Table 13: Comparison between AMSHEV and test data for Case 4

	Specimen 1	Specimen 2	Difference between A & B (%)	Average test data	AMSHEV (2011)	Difference between D & E (%)
	(A)	(B)	(C)	(D)	(E)	(F)
K_E (lb/in)	1403	1729	23.17	1536	1468	4.50
P_{ult}(lbs)	5712	4892	14.36	5302	5061	4.55
$\Delta_{P_{ult}}$ (in)	4.07	2.83	30.47	3.45	3.97	14.98

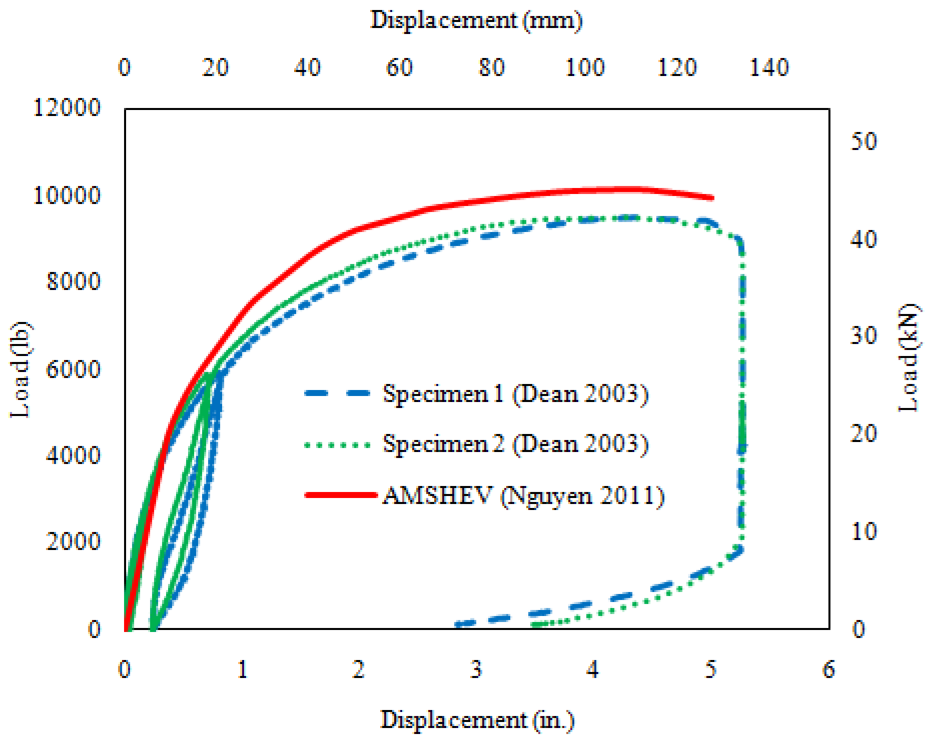

Figure 18: Case 5: With 850 lb/ft vertical load and with hold-down anchor

Table 14: Comparison between AMSHEV and test data for Case 5

	Specimen 1 (A)	Specimen 2 (B)	Difference between A & B (%) (C)	Average test data (D)	AMSHEV (2011) (E)	Difference between D & E (%) (F)
K_E (lb/in)	2181	2235	2.46	2208	2319	5.06
P_{ult}(lbs)	9510	9520	0.11	9515	10130	6.47
$\Delta_{P_{ult}}$ (in)	4.36	4.26	-2.29	4.31	4.27	1.01

4.2 Comparison of Results to Johnston's Model and Dean's Experimental Test Data

Table 15 compares the results between Dean's test data, Johnston's model and the newly proposed model.

Table 15: Comparison between Dean's test data, Johnston's model, and new model results

Load Case	Vertical Load (lb/ft)	Hold-down anchor present	K_E (lb/in), P_{ult}(lb) & $\Delta_{P_{ult}}$ (in)	Average test data (A)	Johnston's model (B)	AMSHEV (C)	% difference between A & C
1	1700	Yes	K_E	2497	3145	2518	0.82
			P_{ult}	10103	6289	9918	0.94
			$\Delta_{P_{ult}}$	4.01	2	3.87	3.49
2	1700	No	K_E	2680	2606	2645	1.29
			P_{ult}	9432	5211	9401	0.33
			$\Delta_{P_{ult}}$	3.52	2	4.46	26.99
3	0	Yes	K_E	1759	3201	1825	3.76
			P_{ult}	7845	6402	8147	3.85
			$\Delta_{P_{ult}}$	4.46	2	4.47	0.15
4	0	No	K_E	1537	2574	1468	4.5
			P_{ult}	5302	2600	5061	4.55
			$\Delta_{P_{ult}}$	3.45	1.01	3.97	14.98
5	850	Yes	K_E	2208	-	2319	5.06
			P_{ult}	9515	-	10130	6.47
			$\Delta_{P_{ult}}$	4.31	-	4.27	1.01

(-): With case 5, Johnston (2005) did not have results from the FE model to compare with Dean's (2004) test data

From Table 15, the following results can be summarized:

1. **Ultimate load**: The new model yields an ultimate load within 5% of the average test results for the first 4 cases, and 7 % for Case 5. This is a significant improvement by 15-50% from the Johnston's model (2005).
2. **Effect of the vertical load on the ultimate load capacity:** The new model also shows the additional benefit of the presence of the vertical load on the ultimate

lateral load capacity, which Johnston's model (2005) did not successfully reveal. For Case 3, when there is no vertical load, but a hold-down anchor is present, Johnston's result even showed a counter-beneficial effect of the vertical load, which is not true according to the experimental test results. With the hold-down anchor, vertical loads (i.e; 1700 lb/ft) increase the ultimate load capacity by 28% as seen from with Dean's data, and 26% with the new FE model data, which exhibits good agreement.

3. **Effect of the hold-down anchor on the ultimate load capacity:** The new FE model also shows the same result as the experimental test data, where the effectiveness of the hold-down anchor is only well demonstrated in the cases without vertical load. This is because the vertical load has a greater effect than the hold-down anchor in its purpose -- to keep the vertical studs from lifting up and reduce the stress inside the studs. Johnston's model did not successfully capture this phenomenon either. When there was no vertical load, the presence of hold-down anchors increased the ultimate capacity by 48% as seen in Dean's test data (2004), and 61% with the new model data. When there was vertical load, the hold-down anchors only increased the ultimate load capacity by 7% with Dean's test data, and 6% with the new model data, again showing good agreement between the experimental test data and new FE model.

4. **Effect of the vertical load on the ductility of the shear wall:** It was observed in Dean's tests that the ductility of the walls decreased as the vertical load was increased. The average experimental test data showed that, with the presence of hold-down anchors, the wall when subjected to 1700 lb/ft vertical load reached

the ultimate load at a displacement of 4.01 in. When subjected to 850 lb/ft vertical load, the ultimate load occurred at a displacement of 4.31 in. Without vertical load on the wall, it reached the peak at a displacement of 4.46 in. The corresponding displacements at ultimate loads in the new model data are 3.87, 4.27 and 4.47 in., respectively, for cases 1, 5 and 3.

4.3 Parametric Study

4.3.1 Effect of Varying Vertical Load on Shear Wall Ductility

As discussed in subsection 4.2, the experimental test data showed that when the vertical load increases, the ductility of the shear wall decreases, and the FE model also revealed the same result. But that was concluded based on only 3 load cases because of the short of available experimental test data. In order to strengthen this conclusion, the FE model was analyzed with two more values of vertical load at 400 lb/ft and 1200 lb/ft, with the presence of a hold-down anchor. All the analyzed results of the FE model with varying vertical load and with a hold-down anchor are shown in Table 16 and Figure 19 illustrates the results in the table. It can be seen from Table 16 and Figure 19 that, the displacement at ultimate load decreases from 4.47 in. to 3.87 in. when the vertical load increases from 0 to 1700 lb/ft, which does reinforce the same conclusion based on observation of the experimental tests.

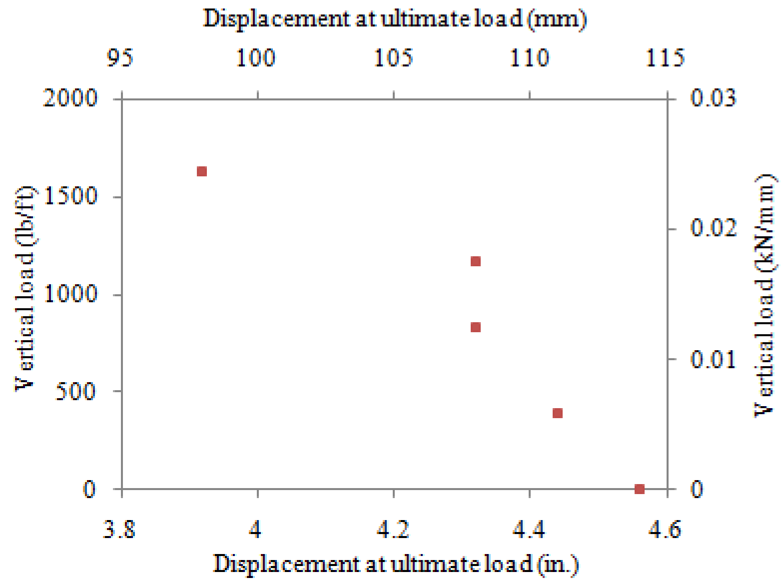

Figure 19: Effect of varying vertical load on shear wall ductility

Table 16: Effect of varying vertical load on shear wall ductility

Vertical load (lb/ft)	Hold-down anchor	FE model data	
		P_{ult}(lb)	Δ_{ult} (in)
0	Yes	8147	4.47
400	Yes	10249	4.37
850	Yes	10130	4.27
1200	Yes	10034	4.27
1700	Yes	9918	3.87

4.3.2 Effect of Varying Vertical Load and Hold-down Anchor on Shear Stress Distribution

As previously discussed in the Chapter III, the vertical load has a beneficial effect on the ultimate load as it keeps the vertical studs from lifting up and also reduces the stress inside the wall. To illustrate, some shear stress contour plots are made to show the effect of the vertical load in reducing the shear stress in the sheathing. All four cases were analyzed with the same value of lateral load of 5057 lbs, which is the maximum load for the Case 4. Figures 20, 21, 22, and 23 show the distribution of the shear stress in the sheathing for all 4 cases. Table 17 compares the maximum shear stress between the cases with and without vertical loads.

Table 17: Comparison of maximum shear stress

Load Case	Vertical load	Hold-down anchor	Maximum shear stress τ_i (psi)	Reduction in comparison with Case 4 (%)
1	1700	Yes	157	30
2	1700	No	179	20
3	0	Yes	192	14
4	0	No	224	0

As can be seen from the Table 17, the vertical load does reduce the maximum shear stress in the sheathing, and the hold-down anchor also has a similar beneficial effect. For the two cases without vertical load, Cases 3 and 4, the hold-down reduces the maximum shear stress by 14%. When is no hold-down anchor, as in Case 2, the vertical load reduces the maximum shear stress by 20%. The addition of the hold-down anchor along with the presence of the vertical load reduces the maximum shear stress by 30%.

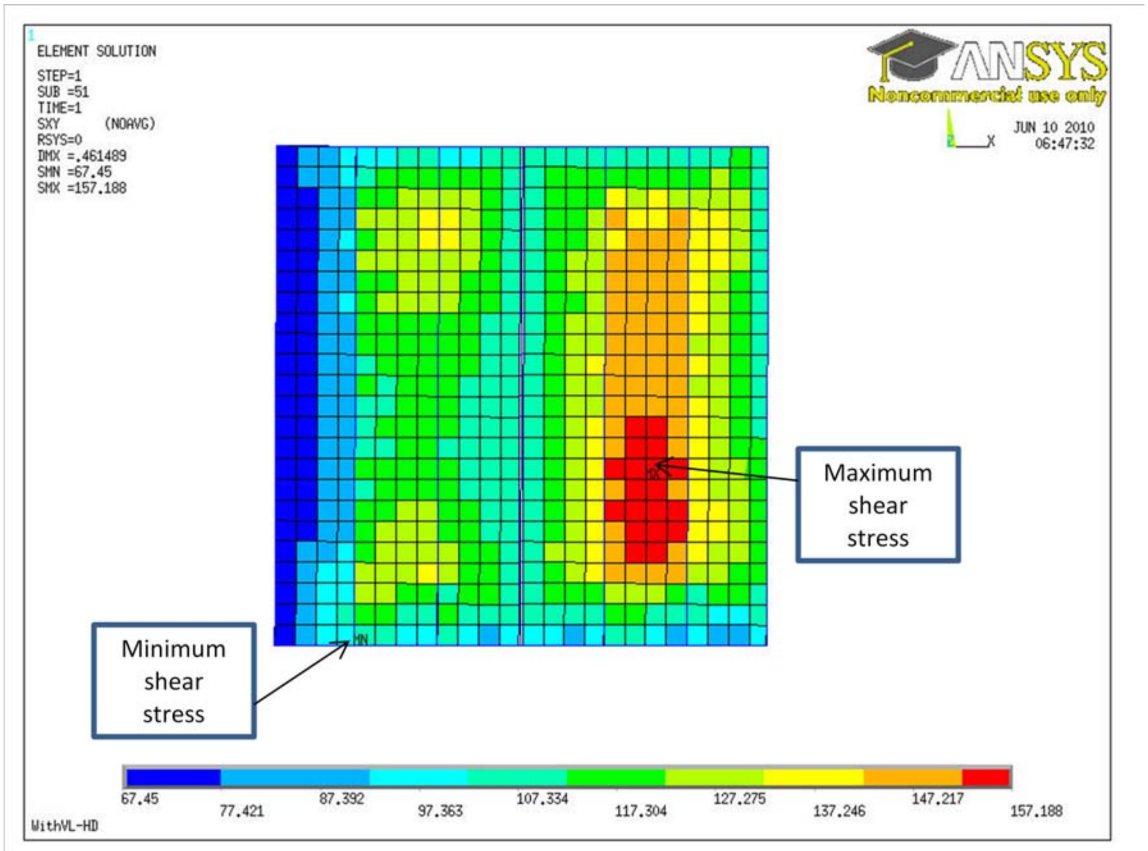

Figure 20: Shear stress distribution for Case 1-with vertical load and hold-down anchor

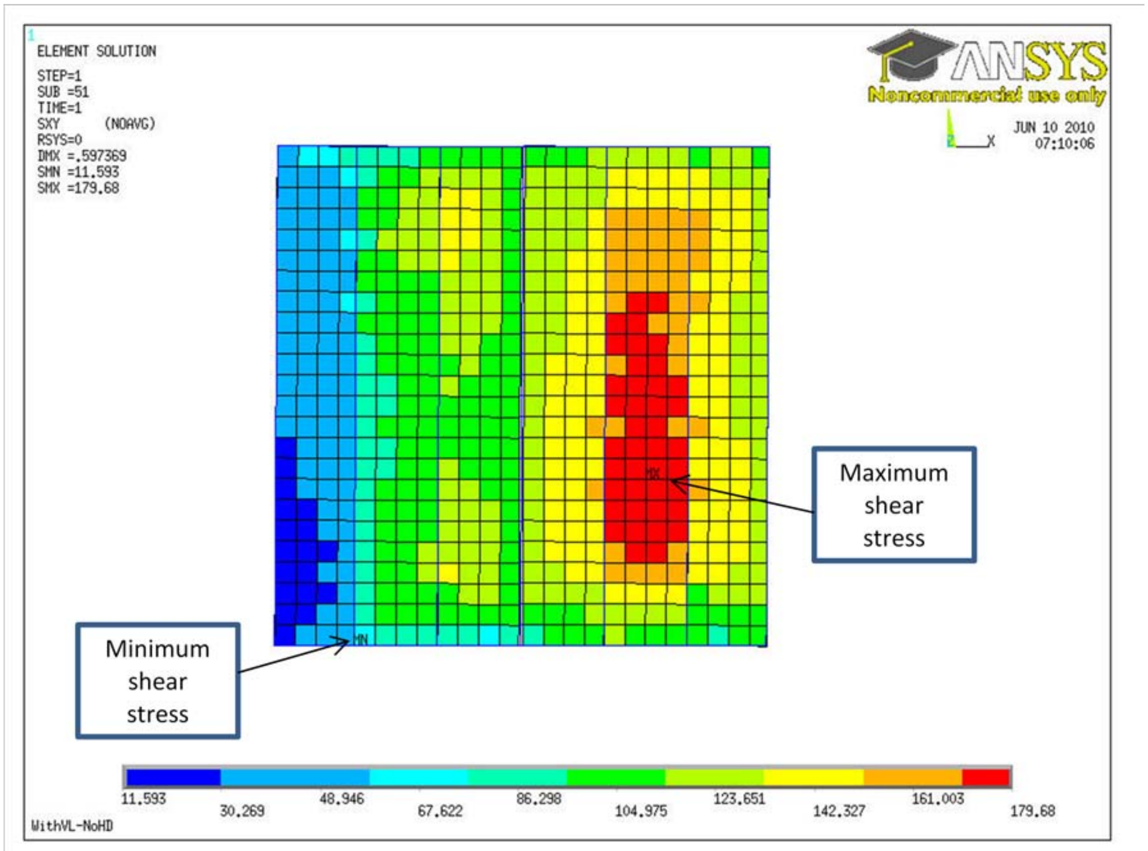

Figure 21: Shear stress distribution for Case 2-with vertical load and no hold-down anchor

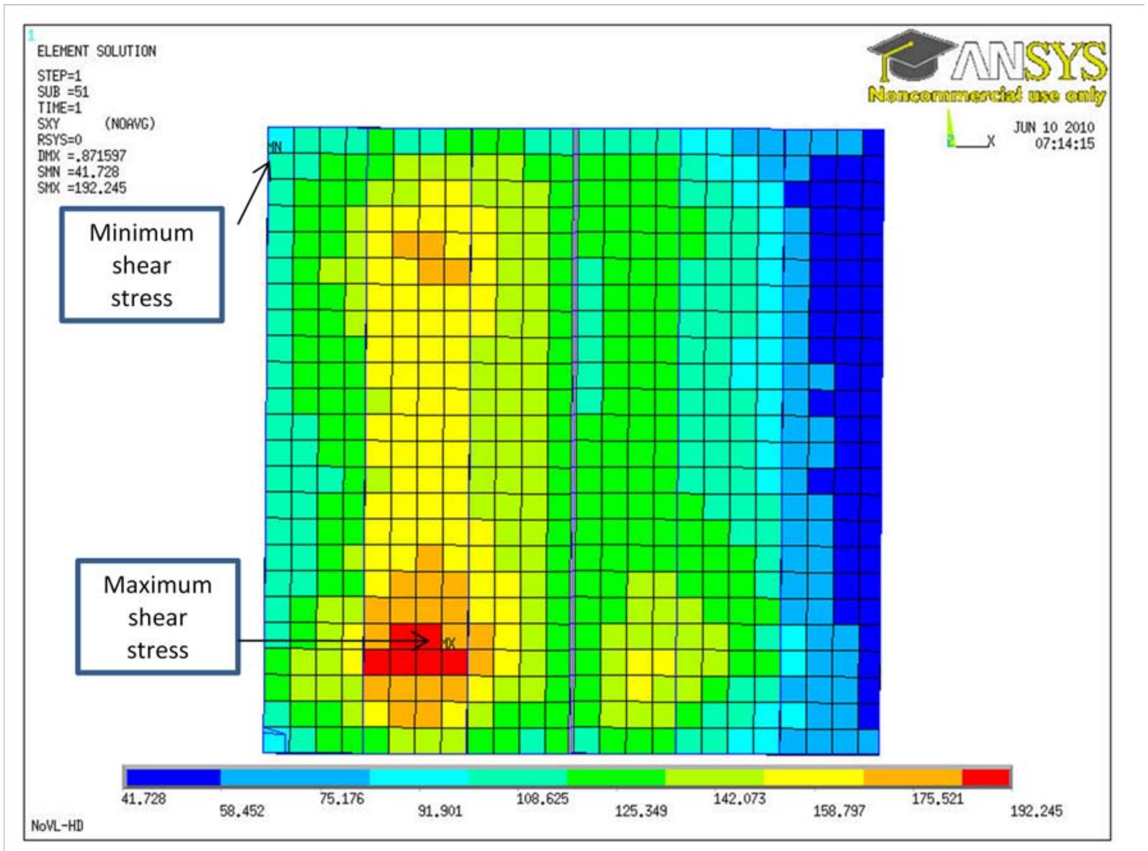

Figure 22: Shear stress distribution for Case 3-no vertical load and hold-down anchor

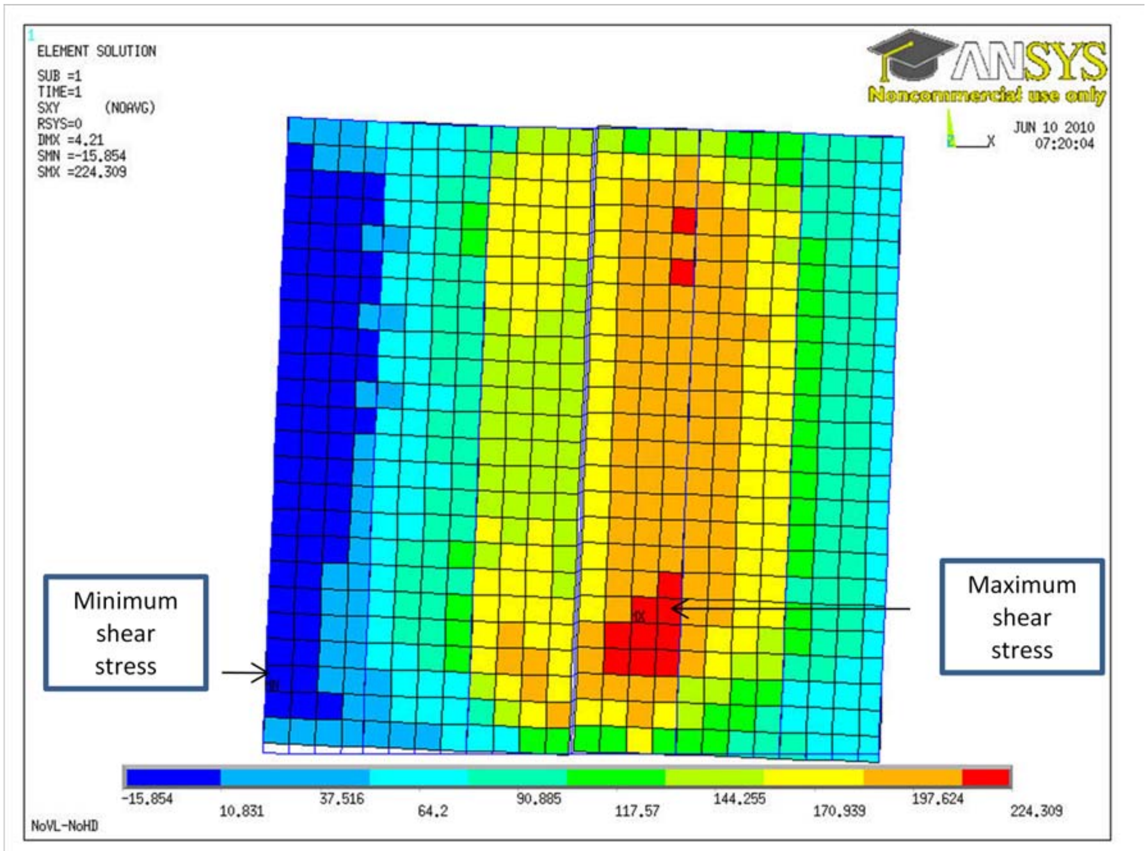

Figure 23: Shear stress distribution for Case 4-no vertical load and no hold-down anchor

CHAPTER V

CONCLUSIONS

5.1 Summary

A new FE model of wood frame shear walls, AMSHEV, has been developed and calibrated against experimental test data to predict the behavior of wood frame shear walls with different magnitudes of vertical load and support conditions. The AMSHEV model accounts for the load-displacement response of nailed wood connections and three major failure mechanisms, which have not been accounted for in previous models or computer programs. Comparison shows good agreement between the model and experimental test data. Based on the results of this study, the following conclusions can be made:

1. **Accuracy**: The new model yields an ultimate load within 5% of the average test results for the first 4 cases, and 7% for Case 5. This is a significant improvement by 15-50% from Johnston's model (2005).
2. **Effect of the vertical load on the ultimate load capacity**: The new model also shows the additional benefit of the presence of the vertical load on the ultimate lateral load capacity as observed in the experimental tests by Dean (2003). With the hold-down anchor, vertical loads (i.e; 1700 lb/ft) increase the ultimate load capacity by 28% as seen from with Dean's data, and 26% with the new model data, which exhibits good agreement.

3. **Effect of the hold-down anchor on the ultimate load capacity**: The new model also shows the same result as the experimental test data, where the effectiveness of the hold-down anchor is only well demonstrated in the cases without vertical load. When there was no vertical load, the presence of hold-down anchors increased the ultimate capacity by 48% as seen in Dean's test data (2003), and 61% with the new model data. When there was vertical load, the hold-down anchors only increased the ultimate load capacity by 7% with Dean's test data, and 6% with the new model dat, again showing good agreement between the experimental test data and the new model.
4. **Effect of the vertical load on the ductility of the shear wall**: It was observed in Dean's tests that the ductility of the walls decreased as the vertical load was increased. The average experimental test data showed that, with the presence of hold-down anchors, the wall when subjected to 1700 lb/ft vertical load reached the ultimate load at a displacement of 4.01 in. When subjected to 850 lb/ft vertical load, the ultimate load occurred at a displacement of 4.31 in. Without vertical load on the wall, it reached the peak at a displacement of 4.46 in. The corresponding displacements at ultimate loads in the new model data are 3.87, 4.27 and 4.47 in., respectively, for Cases 1, 5 and 3.
5. **Applicability:** A commercial, general purpose program like ANSYS© can be used to develop detailed FE models like AMSHEV without having to rely on complex research-based codes to reliably estimate the strength and evaluate the behavior of wood frame shear walls.

5.2 Future Work

The results of analysis suggest some major trends for the future work in order to further investigate the behavior of wood frame shear walls, especially as it relates to additional numerical modeling parametric studies. Future work may focus on cyclic analysis of the FE model of shear walls in order to predict the response of wood frame shear walls under clycic loadings. Additionally, the analytical model of wood frame shear wall can be used in evaluation of multistory buildings. Since no previous experiemental tests have been conducted on shear walls under clyclic loading protocol with vertical load applied, future work may also investigate large-scale experimental cyclic testing of wood frame shear walls with vertical load.

Cyclic analysis of wood frame shear walls: The analysis results of the FE model presented in this thesis are only for static nonlinear loading protocol. In order to characterize the response of wood frame shear walls under cyclic loading protocol, which enables the model to be used for calculation of wood frame shear walls subjected to dynamic loads such as earthquakes, some more work need to be done. Firstly there were limited available experimental test data of wood frame shear walls subjected to cyclic loading protocols. The only load case that has been investigated for cyclic loading is when there is no vertical load, with the presence of hold-down anchors. More experimental tests on shear walls under cyclic loading should be conducted with inclusion of vertical load. This will be the basis to understand the behavior of wood frame shear walls under different load cases for cyclic loading. For the FE model developed in ANSYS©, in order to run cyclic analysis, the nailed-wood connections can be modeled using available elements in ANSYS©, as proposed by Dinehart et al. (2008). Dinehart suggested a model for the nailed-wood connections using two elements in both x- and y- directions, yielding a total of four elements. One of the two elements models secondary cycle response (plastic deformation of the nail and nail/wood friction) and the other models the primary cycle response (cycles with displacements exceeding the maximum observed displacement). All elements can be modeled using COMBIN40 element, which features a combination of springs, damper, friction slider and gap. The response of the connection model for any given cycle is a function of current cycle displacement and previous maximum displacement. The limited ability of this method is that it assumes the connection never fails but rather continues to provide resistance even at very large displacements; consequently, this method cannot be used to predict ultimate load capacity. However, this model of the nail-wooded connection can be applied to an entire large range of motion within the realistic range of design standards.

REFERENCES

AF&PA (2005), *National Design Specification for Wood Construction*.

ANSYS, Inc. (2010), ANSYS© version 12.

Cheung, C. K. Itani, R. Y. and Polensek, A. (1988). "Characteristics of wood diaphragms: Experimental and parametric studies." *Wood and Fiber Science,* 20(4): 438–456.

Dean P.K. (2003). "Experimental investigation of the effect of vertical load on the capacity of wood frame shear walls." Undergraduate Senior thesis, University of Delaware, Delaware.

Dean, P.K. and Shenton III, H.W. (2005) "Experimental investigation of the effect of vertical load on the capacity of wood shear walls," *ASCE J. Struct. Eng.*, 131(7): 1104-1113.

Dinehart, D. W. and Shenton, H. W. III. (1998a). "Comparison of the response of timber shear walls with and without passive dampers." *Proc., Structural Engineering Worldwide*, Paper No. T207-5, Elsevier Science, New York.

Dinehart, D. W. and Shenton, H. W. III. (1998b). "Comparison of static and dynamic response of timber shear walls." *J. Struct. Eng.*, 124(6): 686–695.

Dinehart, D. W. and Shenton, H. W. III. (2000). "Model for dynamic analysis of wood frame shear walls." *J. Eng. Mech.*, 126(9): 899–908.

Dolan, J. D. and Foschi, R. O. (1991). "Structural analysis model for static loads on timber shear walls." *J. Struct. Eng.*, 117(3): 851–861.

Folz, B. and Filiatrault, A. (2001). “Cyclic analysis of wood shear walls.” *J. Struct. Eng.*, 127(4): 433–441.

Gupta, A. K. and Kuo, G. P. (1987). “Wood-framed shear walls with uplifting.” *J. Struct. Eng.*, 113(2): 241–259.

Hite, M.C (2002). “Modeling the nonlinear behavior of wood frame shear walls.” M.S thesis, University of Delaware, Delaware.

Hite, M.C. and Harry W. Shenton III (2002). “Modeling the nonlinear behavior of wood frame shear walls.” *Proc.,15th ASCE Engineering Mechanics Conference*, June, Columbia University, New York.

Itani, R. Y. and Robledo, F. M. (1984). “Finite element modeling of light-frame wood walls.” *Civil engineering for practicing and design engineers,* Vol. 3, Pergamon, Tarrytown, N.Y., 1029–1045.

Itani, R. Y. and Cheung, C. K. (1984). “Nonlinear analysis of sheathed wood diaphragms.” *J. Struct. Eng.*, 110(9): 2137–2147.

Johnston A.R. (2005). “Response of wood frame shear walls with applied lateral load.” M.S thesis, University of Delaware, Delaware.

Seaders, P., Gupta, R. and Miller, T. H. (2009). “Monotonic and cyclic load testing of partially and fully anchored wood-frame shear walls,” *Wood and Fiber Science*, 41(2): 145-156.

White, M. W., and Dolan, J. D. (1995). “Nonlinear shear-wall analysis.” *J. Struct. Eng.*, 121(11): 1629–1635

APPENDIX

Using Ansys via Hydra Supercomputer at TAMU

(by Hai Nguyen Dinh)

Register a Hydra supercomputer account

- Go to https://sc.tamu.edu/ams/ and register an account

Download and install programs for remote accessing using windows

- Download Putty for remote login. Putty can be downloaded free at http://www.chiark.greenend.org.uk/~sgtatham/putty/
- Download and install X-ming for graphics in windows. X-ming can be downloaded free at http://sourceforge.net/projects/xming/
- Download and install WinSCP to transfer files to your Hydra Supercomputer account. WinSCP can be downloaded free at http://winscp.net/eng/download.php

Configuration

- Run Putty program to open its main window. Select SSH for the protocol and enter the host name of the remote machines “hydra.tamu.edu”.
- On Putty Main window, select “connection/SSH/” branch, then make sure the following SSH parameters are correct:
    - Click on “2 only” for preferred SSH protocol version
    - Click on “Auth” portion of the SSH branch, then click on “Attempt keyboard interactive auth” and “Allow agent forwarding”
    - On X11 portion, click on “Enable X11 forwarding”
- Now you have configured all the parameters as we want them, you can go back to the sessions window and click on the "Save" button to save these settings under the session name of "hydra". For future use, just highlight “hydra” session then click open, you’ll have connection to Hydra supercomputer.
- After you click on open, a window with a command line interface will be presented, you can login using your account name and password

Running Ansys program using Hydra supercomputer

- After login hydra supercomputer, on the command window, type “ module load ansys” to set up the Ansys working environment.
- If you want to use Ansys in a conventional Unix line mode, type “ansys”

- If you want to use Ansys with a point-and-click-options window, type “ansys -g”. In this case, **X-ming program must be running for graphics in windows.**
- For more information, type “man ansys” for the Ansys manual, or read “Ansys at a glance” (after existing Ansys)

Transfering a file to your Hydra account

If you want to run your existing file by Ansys program via Hydra supercomputer, you first need to transfer the file to your Hydra account using WinSCP program.

- After you’ve installed WinSCP. Run the program by double clicking its icon.
- On the main window, type the host name “hydra.tamu.edu” ,port number 22, file protocol SFTP and click on “allow SCP fallback”. Then type your hydra supercomputer account name and password.
- In the SSH portion of the GUI, AES encryption should be moved to the top by highlighting it and pressing the "Up" button until it is at the top of the selection policy. Click on version “2 only”
- Click on login now. If this is the first time you have accessed this particular remote machine through WinSCP, you will see the following message:
- Click on yes to proceed, then the main window will be presented
- The left hand side of the main window is your hardware drive in your computer, and the right hand side is your account in Hydra supercomputer. You can copy your file to your account just by highlighting it then hold your mouse and move from the left to the right, a confirmation notice will be presented, then click on copy and the file will be transferred.

For better understanding about Hydra supercomputer and Unix system, see documentation at http://sc.tamu.edu/help/

ANSYS-AT-A-GLANCE

(by Monique Hite Head and Hai Nguyen Dinh)

Access to Ansys. (See more in "Access to Ansys via Supercomputer"-by Hai Nguyen)

- Run X-ming, Putty and type the preoper commands to open Ansys point-and-click window

Opening an existing file

- Go to the Utility Menu (top taskbar) "File" >> "Resume from" (choose file from directory…file will appear on screen).
- Once the file has been opened, to **save the file as a new one**, go to "File/change title", then a new file will exist in your supercomputer home drive account.
- Go to "File/change jobname" to type the name of the results file, which should already be stored in the directory. (Usually I've named the jobname the same as the filename). If you don't change jobname, the saved result will be written to a default database file "file.db" in your hydra account.

Reviewing

1. **Reviewing a model:** Once you've opened a model, you may want to make sure the model is ok, or when editing an existing model that you don't know well, you can review all the elements, nodes, boundary conditions, internal hinges, material types, cross section properties … of all the model:
   - From the Ansys main menu, go to Preprocessor, click on element type, material properties, real constant (the properties for all the element types. Each real constant set will be related to an element type, so see which real constant set is for which element type, you must review the element to see which type, which constant set and which material set been used), to review all the information about the structure.
   - To see the properties of all the element, nodes, lines, etc. go to "Utility menu/list" choose elements or nodes …
   - To see the properties of some specific elements, nodes …Go to Utility menu/list/ by picking. Then a window will appear and you can choose whether to view node or element properties.
   - To review the boundary condition, or all the coupling nodes (for hinges or pined connections), go to list/other/coupling.
2. **Reviewing an analysis**
   - From the ANSYS Main Menu, go to "General Post-processing" >> "Results Summary" (which is a .rst file). A listing of all of the load steps will appear in this section. You can look at each load step individually to look at the deformed shape and/or stresses during a particular load step.
   - By clicking on "List Results" or Plot Results," you can view or plot contours of some of the results at each node. If you wanted to isolate a particular

element type, i.e. all of the spring fasteners, go to "Select" >> "Entities" >> choose "Elements" >> "By Attributes" >> select "Elem type num", where you would then type the corresponding number assigned to all of the spring fasteners. Click "Select All" >> "Apply" >> "Plot". Now just the fasteners are highlighted and the results will just extract the results corresponding to only the fastener elements.

- To view the results through an animation-like viewer, click on "Results Viewer", which is a .pgr file. Running the results through this viewer helps to refresh the results stored in the .rst file (or "Results Summary").
- To view **a time history of the results**, go to "Time-History Postproc". A time-history viewer window will appear.
  - First, define the variables that you would like to extract from the results file, e.g. displacement and load. Time is always the default 1st variable. Click on "Define Variables" >> "Add" from the menu, or click on the (+) symbol on the time-history viewer window. ANSYS will also prompt you to click on the node for which you would like to obtain the specific results.
  - To make a time-history graph, e.g. the load displacement curve, in the **timehistory viewer window** (not in the main menu), highlight the two variables that you want to plot (hold control), then click on the graph symbol on the window.
  - For the detailed values of the variables, click on "List Variables" in the main menu. For a load-displacement plot, NVAR1 and NVAR2 are defined variables 2 and 3 for the plot to display via the ANSYS window.

  - Once you've listed the variables, a pop-up window of the results will appear. If you clicked on "File >> "Copy to Output", the results will appear in the ANSYS dos-window. From there, you can copy and paste results into a graphical application like MS Excel.

Save an analysis

- You can save on the exit of your job. When you save, you can either save just the Geometry, Solution, and/or Loads--it's up to you. I would just click on "Save Everything" to be on the safe side. However, if you wanted to save your work in the interim, click on "Save as" from the Utility Menu. From there, you can save your work into a directory of your choice.

Running an analysis

- Once a filename and jobname are created, you can run the analysis. Note the "Change jobname" is the file for which the results are stored so you should create this before running an analysis. From the ANSYS Main Menu, click on "Solution" >>"New Analysis">> "Solution Control," which is broken down into 3 menus (access the following tabs…Basic, Sol'n Options, and Nonlinear) of importance…

    - 1) Basic tab: Analysis Options (Large displacement static)…Number of substeps (220)…Maximum number of substeps (250)…Minimum number of substeps (200)…select "All solution items" and Frequency "Write every substep."
    - 2) Sol'n Options: Make sure that the Frequency on this second tab is "Write every substep."
    - 3) Nonlinear tab: For nonlinear options, make sure that the "Line search" is "on" and that the "DOF solution predictor is "on for all substeps."
- To apply a load on elements, click on "Apply." From there, you can place the load where desired. Click on "Displacement" to prescribe/constrain a displacement at a node. (You would have to select the node and the direction that is to be prescribed/constrained). To apply a vertical load, click on "Pressure" >> "On beams". Then, actually click on the beams for which the vertical load is to be applied. For a vertical load in the y-direction, the "Load key is 1" and an direction along the x-tangential is "Load key 2". After specifying the load key, specify the magnitude of that surface load pressure (value/length) in "VALI".
- From there go to "Load Step Opts" >> "Output Ctrls" >> "Solu Printout" >> (Item) "All quantities" >> (FREQ) Every substep.
- Next, specify the .pgr file for the results so go to PGR file. The jobname that you typed earlier should automatically appear in the filename slot. If not, respecify the jobname immediately, by going to "Change Jobname." After the PGR filename is displayed, I just select the first three PGR results items (Stress, structural nonlinear data, and contact data). Also, I usually just have for the "average nodal data", use surface and interior data. Finally, click "OK" to accept everything.
- Go back to "Solution" and click on "Nonlinear" for convergence criteria. For my analyses, I had the convergence criteria set at

Label	Ref. Value	Tolerance	Norm	Min. Ref.
F (force)	7500	1e-4	L2	not applicable
U (disp.)	4.00	1e-4	L2	not applicable

- Finally, go to "Solve" >> "Current LS". You will get a warning of 344 due to the springs and the whole deal of coincident nodes. That warning you can ignore, however, if another error propogates, you should reanalyze the model.

Hydra supercomputer account memory limit:

- There is a limited memory for an account at Hydra supercomputer, and this can affect the analysis by Ansys. Since the new data may not be written during ansys running. You can either delete some unimportant files in your Hydra account, or move them to your home computer drive, or you can copy the file to a scratch drive at Hydra supercomputer (which you have 10 GB memory to use), in this case, you must save the analysis and copy the file back to your Hydra home drive or your computer drive after running the analysis, because this is not a long-term drive.

"PlotCtrls"

- You can zoom in/out by clicking on "PlotCtrls" >> "Pan, Zoom, Rotate", by which another pop-up menu will appear, and that task menu is pretty self-explanatory.
- From "PlotCtrls," you can animate the model along with its results (deformed shape, for example). (Animate is midway the menu once you click on "PlotCtrls"). You can also save the animation.
- From "PlotCtrls," you can also view the boundary conditions by clicking on "Symbols" >> "All Applied BCs". Numbering can also be found under "PlotCtrls" above "Symbols."
- From "PlotCtrls", you can capture an image that can be imported into another application.

VITA

Hai Nguyendinh received his Bachelor of Engineering degree in civil engineering from Hanoi University of Transport and Communication in 2005. He entered the Master of Science program at Texas A&M University in January 2009 and received his Master of Science degree in May 2011. His research interests include finite element modeling and bridge engineering. He plans to publish a journal paper on finite element modeling of wood frame shear walls.

Mr. Nguyen may be reached at Hanoi University of Transport and Communication, Lang Thuong, Dong Da, Hanoi, Vietnam. His email address is blueocean_xm@yahoo.com.vn and his mailing address is So 60, To 4, Khu Tan Binh, Xuan Mai, Chuong My, Hanoi 2, Viet Nam.